NASA Technical Memorandum 82978

Uniform Engine Testing Program Phase I: NASA Lewis Research Center Participation

T. Biesiadny, L. Burkardt, and W. Braithwaite
Lewis Research Center
Cleveland, Ohio

October 1982

Work performed for
Advisory Group for Aerospace Research and Development (AGARD)
Propulsion and Energetics Panel

ENTER:

26 1 1 RN/NASA-TM-82978

DISPLAY 26/5/1

83N14126*# ISSUE 5 PAGE 622 CATEGORY 7 RPT#: NASA-TM-82978 E-1407

NAS 1.15:82978 82/10/00 63 PAGES UNCLASSIFIED DOCUMENT

UTTL: Uniform engine testing program. Phase 1: NASA Lewis Research Center participation

AUTH: A/BLESIADNY, T.; B/BURKARDT, L.; C/BRAITHWAITE, W.

CORP: National Aeronautics and Space Administration. Lewis Research Center, Cleveland, Ohio. AVAIL.NTIS SAP: HC A04/MF A01

MAJS: /*ALTITUDE TESTS/*ENGINE TESTS/*GROUND TESTS/*TURBOJET ENGINES

MINS: / AIR FLOW/ INTAKE SYSTEMS/ JET THRUST/ TEST FACILITIES

ABA: S.L.

NASA Technical Memorandum 82978

Uniform Engine Testing Program Phase I: NASA Lewis Research Center Participation

T. Biesiadny, L. Burkardt, and W. Braithwaite
Lewis Research Center
Cleveland, Ohio

October 1982

Work performed for
Advisory Group for Aerospace Research and Development (AGARD)
Propulsion and Energetics Panel
Subcommittee 01 (Airbreathing Engine Testing and Test Facilities)
Working Group 15

NASA

Trade names or manufacturer's names are used in this report for identification only. This usage does not constitute an official endorsement, either expressed or implied, by the National Aeronautics and Space Administration.

PREFACE

Presented herein is a summary of the results of tests conducted at the NASA Lewis Research Center, Cleveland, Ohio, U.S.A. as part of the AGARD Uniform Engine Testing Program. The format used for the report is that specified in the Uniform Engine Testing Program General Test Plan, dated January, 1982.

TABLE OF CONTENTS

NOMENCLATURE

The nomenclature used in this report is consistent with the nomenclature specified in the Uniform Engine Testing Program General Test Plan, dated January, 1982. Any terms which have not been defined in the General Test Plan are defined in the report as they are used.

1.0 INTRODUCTION

The Propulsion and Energetics Panel, Working Group 15, of the Advisory Group for Aerospace Research and Development (AGARD) is sponsoring a Uniform Engine Testing Program (UETP). In this program, two jet engines will be tested under identical conditions in a variety of altitude and ground level facilities as a means to correlating these facilities.

The general test objectives of the UETP, as stated in the General Test Plan (ref. 1), are the following:

- To provide a basis for upgrading the standards of turbine engine testing within AGARD countries by comparing test procedures, instrumentation techniques, and data reduction methods, thereby increasing confidence in performance data obtained from various engine test facilities.
- To compare the performance of an engine measured in ground-level test facilities and in altitude facilities at the same nondimensional conditions and establish the reasons for any observed differences.

NASA Lewis Research Center was responsible for initiation of the UETP. It was responsible not only for its own hardware, instrumentation, and operational costs but also for initial program management and procurement of some hardware and instrumentation for use in the remaining phases of the UETP.

Presented herein is a report on the results of testing two J57-19W turbojet engines in an altitude test facility at NASA in support of the AGARD panel's efforts.

2.0 APPARATUS

This section describes briefly the major items of the test installation at NASA, namely, the facility, engines, bellmouth, inlet ducting, modified tailpipe-nozzle assembly, compressor bleed, oil cooler, engine inlet bullet nose, fuel, and instrumentation.

Hardware and instrumentation used for the NASA phase of the UETP which were made available for use by other participants in the program are listed in the General Test Plan (ref. 1). It was the responsibility of each UETP participant to ensure that any hardware or instrumentation used in its engine test facility met the operational and safety requirements for that facility.

2.1 Facility

A NASA Altitude Test Facility, the Propulsion Systems Laboratory test cell 3 (PSL-3), was utilized for the UETP. The engine installation in this test cell, a conventional direct connect type, is shown photographically and schematically in figure 1. In the UETP installation, the engine was mounted in a "dog house" test stand mounted on the thrust bed.

The thrust bed was suspended by four flexure rods attached to the chamber supports and was free to move except as restrained by a

dual load-cell system that allowed the thrust bed to be preloaded and the thrust force to be measured.

The test cell included a forward bulkhead, which separated the inlet plenum from the test chamber (7.3 m diam). Air of the desired temperature and pressure flowed from the plenum through the bellmouth into the inlet duct. A labyrinth seal was used to isolate the inlet ducting from the bellmouth which was attached to the bulkhead. The inlet ducting, which was mounted on the thrust bed, was mated to the engine through an inflatable seal to minimize loading on the engine front flange.

Engine exhaust gases were captured by a collector, which extended through the rear bulkhead, thereby minimizing the possibility of exhaust gas recirculation into the test chamber.

2.2 Test Article

2.2.1 Engines

Two J57-19W nonafterburning turbojet engines, (S/N 607594 and 615037 hereafter referred to as engine 1 and engine 2, respectively) were furnished by the US Air Force for the UETP. The basic J57 engine (refs. 2 and 3), a schematic of which is shown in figure 2, is a two-spool axial flow machine with a nine-stage low pressure compressor, seven-stage high pressure compressor, cannular combustor, single stage high pressure turbine, two-stage low pressure turbine and fixed convergent nozzle with a tail cone extending through the nozzle exit plane. The only variable feature is the intercompressor bleed which discharges air overboard during starting and low power operation.

2.2.2 Bellmouth and Inlet Ducting

The bellmouth and inlet ducting (shown in fig. 1) including the inlet airflow station, station 1, are typical of the inlet hardware used in NASA altitude test facilities. The inlet ducting from the airflow station to the engine inlet, station 2, consisted of a conical spool piece ($5^{\circ}23'$ half angle) for the transition from the smaller diameter at station 1 to the larger diameter at station 2, constant diameter ducting, a seal to minimize loads on the engine inlet flange, and an engine inlet instrumentation spool piece.

2.2.3 Modified Tailpipe and Reference Nozzle

Following from the fact that the tailcone on the standard J57 extends through the nozzle exit plane (see fig. 2), the Bill of Material (BOM) nozzle was replaced by a cylindrical tailpipe and a convergent nozzle (strengthened as required), both fabricated by rolling sheet metal. The BOM nozzle and the cylindrical tailpipe with the convergent

nozzle are shown in figure 3. It was anticipated that the cylindrical tailpipe would not only produced a more uniform nozzle inlet flow profile but also provided a more suitable platform for the pressure and temperature instrumentation needed to establish nozzle inlet conditions. While the latter goal was accomplished, the former met with only partial success (see section 3.2.1). This approach, however, did require a calibration test run with the new tailpipe-nozzle assembly to size the nozzle so that engine performance could be restored to approximately the nominal value. The nozzle calibration sequence is outlined in Appendix A. Even though two engines were available for the program, only one tailpipe-nozzle assembly was used.

2.2.4 Compressor Bleeds

The production engine configuration (J57-19W) utilizes two compressor bleed valves (left and right sides). Operation of the engine with the bleed valves in this configuration, however, limits the high-power bleeds closed speed range. To expand this speed range, the right-hand bleed port was capped and the left-hand bleed port enlarged to an acceptable alternative configuration as described in the General Test Plan (ref. 1). In addition, anti-icing and customer bleed ports were capped at suitable locations.

2.2.5 Oil Cooler

Following from the fact that the engine operation required the use of an external oil cooler (an aircraft part), a test stand mounted oil cooler was used and shipped with the engine. This oil cooler, which used water as the coolant, was set to maintain the oil temperature at 367 ± 6 K at the outlet of the oil cooler. No attempt was made to perform heat transfer calculations.

2.2.6 Engine Inlet Bullet Nose

The engine inlet bullet nose, which is an aircraft rather than an engine part, was fabricated from existing designs (see ref. 1). This part was then modified to permit pinning of the engine inlet instrument rakes.

2.2.7 Fuel

Jet A fuel rather than JP4, the most commonly used fuel for this engine, was used for the UETP necessitating a one-time engine re-trim of both engines at NASA.

2.3 Test Instrumentation

The instrumentation package was divided into two categories, namely, facility-peculiar, or primary instrumentation, and engine-peculiar, or reference instrumentation, both of which will

be discussed in more detail herein. The primary instrumentation was that used to measure those parameters which were used to calculate inlet total airflow, net thrust and specific fuel consumption (SFC)(see Appendices B, C, and D for details of the calculations). The reference instrumentation, which was used to set test conditions, monitor engine health and record any engine deterioration, consisted of pressures and temperatures at the engine inlet, high compressor discharge, turbine discharge and exhaust nozzle inlet, exhaust nozzle trailing edge statics, speed sensors, turbine type fuel flow meters and associated thermocouples, vibration pickups and pressures and temperatures to monitor the test cell environment and oil condition.

The locations for the majority of the instruments are shown schematically in figure 4. With regard to this figure, it should be noted that the numbering system used to identify engine stations (not the one traditionally assigned to this engine) is in agreement with the SAE recommendations as listed in reference 4. Steady state instrumentation (insensitive to time-rate variance above 2 Hz) was used for the UETP except for the high response (0 to 500 Hz) static pressures (Kulite Model XTL5-140-5D) needed to evaluate the turbulence characteristics of the engine inlet airflow and transient instrumentation (0 to approximately 5 Hz) used to measure selected engine-test cell parameters to verify stable engine-test cell conditions. Finally, all temperatures were measured with Chromel-Alumel thermocouples.

Brief comments follow on the choice of some of the reference instrumentation. The engine inlet instrumentation was needed to set inlet conditions as well as to determine circumferential and and radial pressure and temperature profiles and the level of time variant pressure fluctuations.

Boundary layer rakes were required at station 2 because boundary layer thickness was expected to vary with each installation. It was assumed that this boundary layer thickness would affect average engine inlet pressure and compressor performance.

Instrumentation was available for use at the high pressure compressor discharge. The information from this instrumentation was used to make some of the component performance calculations.

Engine health monitoring instrumentation such as that used to measure vibrations, oil breather pressure, etc., is not shown in figure 4.

3.0 TEST DESCRIPTION

3.1 Test Conditions and Procedures

The description of the test conditions and procedures is divided into two parts: (1) preliminary tests such as those needed for the modified tailpipe-nozzle adjustments and for determination of thrust calibration terms and (2) the test points (see Table I)

which are to be duplicated by the altitude facilities participating in the UETP.

3.1.1 Preliminary Tests

The engines were retrimmed, before preliminary tests, with Jet A fuel and run a sufficient number of hours to minimize performance shifts during breakin.

3.1.1.1 Modified Tailpipe-Nozzle Adjustments

The BOM engine was equipped with a tail cone that extends through the nozzle exit plane necessitating that a cylindrical tailpipe and convergent exhaust nozzle be fabricated and used during the UETP tests. The performance of the modified engine was restored to approximately the performance of the BOM configuration as determined in the altitude test cell through engine calibration with the convergent nozzle as outlined in Appendix A.

3.1.1.2 Determination of Thrust Calibration Terms (NASA Specific)

Tests were performed, as explained in Appendix B, to determine engine-facility related calibration factors such as the forces acting on the thrust stand when loads were applied and drag (i.e., force acting in a direction opposite to the jet thrust force) terms associated with air passing through the inlet ducting labyrinth seal and cell cooling air, if any, impinging on the engine. Thrust bed thermal expansion was not included in the correction terms because it was assumed to be negligible since there was no afterburner operation and cooling air was used to limit the temperature rise in the test cell. In addition, the thrust load cells, which were water jacketed to maintain constant temperature, were located in such a manner as to minimize the effects of thermal expansion.

3.1.2 Test Conditions (UETP Participants)

Table I contains a list of test conditions for the altitude facilities involved in the UETP. NASA's response to this choice of test conditions is discussed below.

3.1.2.1 Ram Ratio of 1.0

It was recognized that conditions near sea level static had to be simulated in the altitude facilities in order that sea level facilities

involved in the program could compare data at similar conditions. However, since these conditions could not be easily simulated in NASA's altitude test facility some adjustments in the test conditions were made as will be explained in section 4.0, TESTING RESULTS.

3.1.2.2 Test Procedure

The general test procedure presented in the General Test Plan (ref. 1) was followed as described below

1. The engine was lit in the usual manner.

2. Inlet and test cell conditions were set as specified in Table I with a tolerance on inlet and cell pressure of ±1% and on inlet temperature of ±3° C.

3. These conditions were maintained as constant as possible while the test was in progress.

4. A suitable number of different throttle settings were selected observing the rules below. The data from these points (two scans* were produced for analysis at each throttle setting) were used to generate a curve such as that shown in figure 5. The Random Error Limit of Curve Fit, RELCF, for this curve was requested to be within a tolerance of ±1% for the data to be considered valid. (The techniques which were used to curve fit the data and determine the RELCF are described in ref. 5.). Figure 6 shows a typical progression of RELCF as the number of throttle settings increased.

5. The following rules were applied:

   (a) Nine throttle settings were distributed, unless restricted by rule (b), as illustrated below.

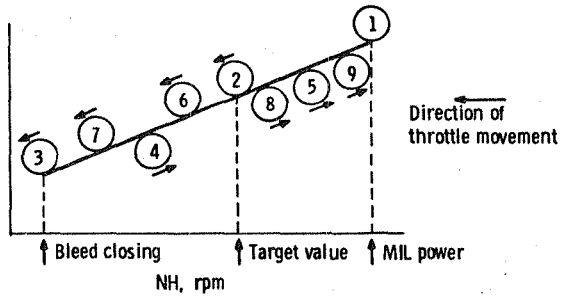

*At NASA, each scan represented data averaged from 20 samples with each sample taken at 1 second intervals.

(b) The throttle settings were restricted to cover the continuous part of the curve from bleed closing to the military power setting (i.e., low pressure turbine discharge temperature of 883 K or power lever angle of 90^{o}, whichever came first). In the rare instances that the bleed opened as throttle setting 3 was approached (e.g., due to bleed system hysteresis), the throttle was advanced toward setting 2 and then returned to a setting slightly higher than the desired 3 setting.

6. A suitable settling period (5 min) was allowed after changing engine conditions. Specifically, the clock was started when the engine operator removed his hand from the throttle after setting the desired high rotor speed. Data recordings were then made with an interval of 2 minutes between each scan.

3.2 Corrections

It was necessary to correct the station 7 pressure measurements and to check the validity of assumptions made in the calculation of the inlet total airflow at station 1 (see Appendix C). The actions taken in connection with these two items are described herein.

3.2.1 Station 7 Measurements

Initial indications were that the station 7 total pressure, P7, was too low when compared with other engine data. After a detailed investigation, this discrepancy was found to be the result of two factors, a calibration error and an improperly weighted P7 average. The calibration error was found in the reference pressure measurement for the Scanivalves used to measure P7. A calibration correction was made to all station 7 total pressure data. The final data package contains these corrections. The initial positions of the station 7 instrument rakes were such that none of the rakes adequately defined the flow nonuniformities caused by the turbine exit struts. The tailpipe and thus the rakes were rotated 12.5^{o} counter clockwise to the "final" position (i.e., the position for the remainder of the UETP at NASA and at other participating facilities). This rotation resulted in an increase in the P7 values and also a minor change in the station 7 temperatures. While the problem of an improperly weighted average was not completely eliminated, the rotation did result in more reasonable nozzle coefficients as will be discussed in section 3.2.2.

All the data obtained with the second engine and all but conditions 5, 6, and 10 for the first engine were with the rakes in the final position.

3.2.2 Inlet Total Airflow Calculation

As described in Appendix C, the method used by NASA to calculate inlet total airflow was dependent on the assumption that the static pressure profile across the inlet duct at station 1 was constant and, as a first approximation, equal to the wall static pressure. A second assumption was that the free stream total pressure was constant and equal to the measurement recorded at the last probe on the boundary layer rakes (i.e., the probe that extended into the freestream).

Surveys of the station 1 freestream total and static pressure profiles were made at selected freestream Mach numbers to document these profiles. Also, a potential flow field computer program was exercised using the UETP inlet geometry and selected inlet conditions. The survey showed a negligible change in total pressure across the free stream (i.e., less than 0.5 cm of water) for freestream Mach numbers from 0.15 to 0.60. The static pressure, however, did show a slightly larger pressure difference between the wall and freestream positions. The potential flow field program also showed a slight static pressure profile.

Following from the above information, the preliminary airflow and related data were revised to include the refined flow coefficient at station 1. This flow coefficient, CD1, plotted as a function of Reynolds Number Index is shown in figure 7.

Evidence that the tailpipe rotation and the inclusion of the refined station 1 flow coefficient were at least satisfactory can be seen in figure 8, a plot of nozzle coefficients against nozzle pressure ratio. In this figure, data from the two highest nozzle pressure ratio conditions show reasonable magnitudes and trends (i.e., both coefficients are less than 1.0 and CG8 is less than CD8).

3.3 Data Reduction

The details of the data reduction package used by NASA for the UETP were furnished to the Working Group Chairman and have been incorporated as part of the General Test Plan (see ref. 1, section 9.0). Additional details of the net thrust, airflow, and fuel flow calculations can be found in Appendices B, C, and D, respectively, of this report.

The thermodynamic properties routines used by NASA can be found in reference 6. Bad data or outliers were detected through a visual inspection of representative data readings from each test period and tagged - the tag being carried through to the data tape. The bad data was then eliminated from the averaging routines and/or

further calculations. When the engines and hardware were shipped from NASA, the instrumentation identified as T7N19 was unserviceable while T7N01, T7L19, and T7I28 were suspect.

The digital data acquisition and processing system available at NASA for the UETP is shown in block diagram form in figure 9. On-line or real time monitoring of the engine tests was accomplished with the altitude test facility computer, a SEL 8600, with its capacity to update individual data channels and calculated parameters once per second. Selected data channels and calculated parameters were available for display on CRT's and were available as line printer output at the test facility. Off-line, or batch, data were processed on an IBM 3033 machine which can produce output on microfiche, line printer paper or magnetic tape. Data will be transmitted upon request to the participating facilities on magnetic tape supplied by the requesting facility along with a summary of each data point, printed on either microfiche (preferred) or line printer paper after the Chairman of Working Group 15 has approved their release. The format will be that specified in the General Test Plan (ref. 1). The final data package forms section 5.0 of this report.

3.4 Uncertainty/Precision of Measurement

An important consideration in evaluating the data in addition to the determination of engine and component deterioration (discussed in section 4.0) is an estimate of the measurement uncertainties associated with the three primary parameters of airflow, net thrust and specific fuel consumption. The ingredients used to determine the final uncertainties are presented in Table II and Appendix E. The results at or near the target high rotor corrected speed of 8900 rpm at each condition are shown in Table III. In addition, a comparison of facility and engine fuel flow meters which shows that all the data fell within a ± 1 percent tolerance band is presented in figure 10.

Generally, the trends were the same for data from both engine tests. That is, the uncertainties were lowest at the highest inlet pressure, 82.7 kPa, but increased to the highest levels as the inlet pressure decreased to 20.7 kPa. Uncertainties for SFC are less for the engine 2 data because one of the two high range facility flow meters was replaced after engine 1 results were reviewed. The precision error for this meter was found to be higher than desired, so the meter was replaced before the start of engine 2 tests.

The two conditions at which this investigation was made which were of specific interest to the Working Group were conditions 3 (condition 5 was substituted for condition 3 for engine 1 at NASA because the latter was not run) and condition 9 (see Table I).

For engine 1, total uncertainty for conditions 5 and 9 (see Table III) were 0.8% and 2.9% for airflow while for net thrust the total uncertainties were 0.6% and 2.3% and for SFC were 1.4% and 2.4%,

respectively. For engine 2, total uncertainty for conditions 3 and 9 (see Table III) were 0.9% and 3.0% for airflow, 1.2% and 2.3% for net thrust, and 1.4% and 2.6% for SFC, respectively.

A cursory look at the level of turbulence at the engine inlet was made, using the high response static pressure measurements at that location (fig. 4), since this could be a factor in the facility-to-facility comparisons. As shown in a typical plot, figure 11, the turbulence level as determined by the root-mean-square of one of the static pressure signals, over a range of frequencies from 0 to 1000 Hz, was less than 2% of the average total pressure. Generally, the turbulence was highest at the lower throttle settings and decreased as the throttle was increased to the military power setting.

4.0 TESTING RESULTS

4.1 Techniques Used for Data Analysis

Following from the fact that a large amount of data were generated during the two engine tests a technique had to be found to present the test results in a meaningful way. It was decided, subject to the approval of the AGARD Working Group sponsoring the UETP, to display the results as described herein.

Appropriate data from each of the ten test conditions for the two engines were first plotted against corrected high compressor rotor speed (i.e., the mechanical speed corrected to standard Sea Level Static (SLS) conditions of 288.17 K and 101.32 kPa) since that was the engine parameter used in setting test conditions. Typical of this type of plot is the illustration in figure 12. These data were represented by a quadratic equation determined through a least square curve fit using the techniques described in reference 5. The next step was to use the coefficients from the quadratic equation and the corrected high compressor speed target value of 8900 rpm to determine the corresponding dependent variable. This dependent variable for each of the ten conditions for each engine was then used for the data analysis that will be presented below. The above technique was repeated for corrected net thrust and corrected specific fuel consumption (SFC) as well as the previously mentioned corrected airflow.

The data presented were corrected to standard SLS conditions rather than the so-called desired conditions as presented in Table I since this would seem to make the task of comparing altitude test facility and ground level test bed data simpler. However, data corrected to the desired conditions are available in the final data package should the Working Group prefer that type of presentation.

4.2 Results

This discussion of test results will be divided into two separate sections with each of the sections covering one engine. This should simplify the comparison of test results between facilities

if it is decided to limit the facility comparisons to a single engine. In the individual sections, the analysis will center on the variation of each of the three major parameters of interest (i.e., airflow, net thrust and specific fuel consumption) with inlet temperature, inlet pressure and ram pressure ratio. This seems to be the most logical approach since these were the three parameters used to set test cell conditions in the altitude test facility.

The discussion of the test results which are presented in figures 13 through 23 for engine 1 and in figures 24 through 33 for engine 2, will be limited in nature, however, until a more thorough investigation of the data has been accomplished by the Working Group. Note that the data are plotted as a ratio of a base value. This base value is defined as that value which was determined at the condition where inlet temperature was 288 K, inlet pressure was 51.7 kPa, and ram pressure ratio was 1.3.

4.2.1 Engine 1, S/N 607594

4.2.1.1 Airflow

Inlet temperature variation and its influence on airflow, were investigated in test conditions 1, 2, and 4 (see Table I). The inlet temperature was calculated using the arithmetic average of the ten thermocouples located at the engine inlet, station 2 (see fig. 4 for a layout of the instrumentation).

It should be remembered that the curve shown in figure 13 represents data at the target value of corrected high rotor speed equal to 8900 rpm for conditions 1, 2, and 4. The target values, in addition, were obtained from a least squares curve fit of the actual test data recorded at the nine engine speed settings between bleeds closed and military power as described in section 3.1.2.2.

A second set of data with inlet temperatures the same as those specified in Table I for conditions 1, 2, and 4, but with the ram ratio increased by lowering the test cell pressure while leaving the inlet pressure unchanged was obtained but not presented here since it is not a part of the UETP requirements. The higher ram pressure ratio conditions were investigated because it was discovered that at the lower condition (i.e., ram pressure ratio = 1.0) exhaust gases recirculated through the test cell bypass line to the inlet plenum. The pressure in the exhaust plenum, which is also the terminus of the bypass line (see fig. 1), was higher than the inlet plenum pressure because of a pressure rise across the exhaust collector. The result was that hot gases leaked past the valve in the bypass line and eventually reached the engine inlet by way of the inlet plenum. Carbon traces at the engine inlet led to the belief that the resultant temperature distortion was

limited to approximately a 45° sector at 315°. This location, as can be seen in figure 4, included one of the two engine inlet thermocouple rakes - a situation which led to an improperly weighted average inlet temperature. If a corrected weighting routine, different from that shown in the UETP General Test Plan, were used to calculate station 2 temperature, the difference between this temperature and the reported temperature would be within 3° C as shown in figure 14.

Figure 13 shows almost negligible variation of corrected airflow ratio as a function of inlet temperature as inlet pressure and ram pressure ratio were held constant. In fact, the variation that is shown may be the result of inlet temperature distortion. The data recorded at the higher ram pressure ratio do not show this variation.

Inlet pressure variation from 82.7 to 20.7 kPa and its influence on corrected airflow was evaluated in test conditions 6, 7, 8, and 9 (see Table I). Engine inlet pressure was calculated using the arithmetic average of the 20 total pressure probes, 5 each on the rakes located at 0°, 90°, 180°, and 270° (see fig. 4).

Figure 15 shows the variation in corrected airflow with the reciprocal of inlet pressure as inlet temperature and ram pressure ratio were held constant at 288 K and 1.3, respectively. The curve fit extrapolation beyond the reciprocal of 82.7 kPa or 0.012 kPa^{-1} is hampered by the lack of data at or near sea level pressure, 101.3 kPa, and thus the curve is less accurate beyond the highest pressure at which data were recorded. Comparison of the curve in figure 15 with that generated by the altitude test facilities which are capable of testing at or near SLS conditions should improve the extrapolation. The decrease in the corrected airflow ratio as the reciprocal of P2AV increases is most likely due to Reynolds number effect. The Reynolds Number Index was approximately 0.5 at 0.02 kPa^{-1} and decreased to nearly 0.2 at 0.048 kPa^{-1}. The corresponding corrected airflow ratio change was a maximum of -3.5%. The two data points at 0.012 kPa^{-1} are the repeat test conditions run as part of the deterioration check. Finally, the ratio at the base condition is not 1.0 because of the curve fit through all the data points.

Ram pressure ratio was calculated by dividing the average engine inlet pressure by the test cell ambient pressure. The test cell ambient pressure was defined as the arithmetic average of the four nozzle external static pressure measurements at the location 1.3 cm forward of the nozzle exit plane (station 0.5 in fig. 4).

As can be seen from Table I, those conditions under which ram pressure ratio was changed as inlet temperature (288 K)

and pressure (82.7 kPa) were held constant were test condtions 3, 5, 6, and 10. For engine 1, NASA ran this series of test conditions at ram pressure ratios of 1.07, 1.3, and 1.7 (i.e., conditions 5, 6, and 10) only.

Figure 16, a plot of corrected airflow ratio against ram pressure ratio with inlet temperature and pressure held constant, shows little or no change in corrected airflow with ram pressure ratio. This is to be expected since the inlet pressure and temperature were held constant at the same time that exhaust nozzle pressure ratio was at or near choked condition for the target value of corrected high rotor speed of 8900 rpm. The ram pressure ratio of 1.0 was not attempted with engine 1 but the curve was extrapolated to that point and shows a decrease in corrected airflow of less than 0.1% from the base value.

4.2.1.2 Net Thrust

The variation of net thrust with inlet temperature, inlet pressure and ram pressure ratio is presented in figures 17, 18, and 19.

The change in the corrected net thrust ratio shown in figure 17 appears to be largely due to the effects of temperature distortion discussed previously with regard to airflow.

In figure 18, where corrected net thrust ratio is plotted against the reciprocal of inlet pressure, the data extrapolated beyond the reciprocal of 82.7 kPa or 0.012 kPa^{-1} again are subjected to question because of the lack of data near the SLS condition as was the case with the data plotted in figure 15. The change in corrected net thrust is due to the unaccounted for terms in the normalization procedure such as Reynolds number effects. Again, a slight difference exists between the actual data at the reciprocal of 51.7 kPa or 0.019 kPa^{-1} and the curve because of the curve fitting technique.

Figure 19 shows a large decrease in corrected net thrust as ram pressure ratio increased. The change was from a +12% at the lowest ram pressure ratio tested (i.e., discounting the extrapolation from ram pressure ratio of 1.07 to 1.0 for reasons previously stated) to approximately a -4% change at the highest ram pressure ratio, 1.7. The ram pressure ratio change from 1.07 to 1.7 resulted in a 26% increase in gross thrust but this increase was negated by an even greater percentage increase in the ram drag term. Thus, a large decrease in net thrust resulted.

4.2.1.3 Specific Fuel Consumption

The variation of SFC with inlet temperature, inlet pressure and ram pressure ratio is presented in figures 20, 21, and 22.

Figure 20 shows an increase in corrected SFC ratio with increase in inlet temperature as inlet pressure and ram pressure ratio were held constant. The corrected SFC change was approximately 2 percentage points from 253 to 308 K.

Figure 21 shows the change in corrected SFC ratio with the reciprocal of inlet pressure as inlet temperature and ram pressure ratio were held constant. It should be noted that the data beyond the reciprocal of 82.7 kPa or 0.012 kPa^{-1} represent an extrapolation. It is anticipated that this extrapolation will change when SLS data are available for trend analyses. It is further expected that these data will also influence the curve fit for data at and below the reciprocal of 82.7 kPa because of the current scarcity of data. Changes in corrected SFC ratio with inlet pressure and temperature are again due to inadequacy of the normalization procedure (i.e., unaccounted for terms in the dimensional analysis).

The data presented in figure 21 show the same general trend as that presented in figure 18 for corrected net thrust except that the former plot shows a much greater change with pressure than the latter plot. A review of the data revealed a significantly larger decrease in corrected fuel flow from the low pressure, 20.7 kPA, to the high pressure, 82.7 kPA than was seen for the corrected net thrust ratio. The result, shown in figure 21, was a variation in corrected SFC from +9% to -2% about the base values.

In figure 22, corrected SFC ratio is plotted against ram pressure ratio for conditions where inlet pressure and inlet temperature were held constant. The trend shown was the result of a small change in corrected fuel flow ratio but a large change in corrected net thrust. This was not unexpected because the inlet pressure and temperature were held constant for the conditions represented in figure 22.

4.2.1.4 Engine and Component Deterioration

An important consideration in the comparison plots between facilities will be the magnitude of the engine deterioration. Toward this end, NASA ran the identical condition as the first and last test conditions (i.e., conditions 6 and 6A in Table I). Before making comparisons, it should be noted that approximately 5 hours were accumulated on the engine between the time it was received and the first time condition 6 was run. This time

was spent trimming the engine for Jet A fuel, cutting the reference nozzle to size and conducting facility calibration tests. This involved numerous excursions between idle and military power and return using slow throttle movements. Further, no emergency conditions occurred during any of the testing with this engine that required rapid throttle movements. No high vibrations were encountered during this preliminary testing nor were they encountered at any time during conduct of the UETP test conditions. The maximum turbine discharge temperature, T5, was kept at or below 883 K. No stalls were indicated by the high response instrumentation used as stall detectors nor were there any audible indications of surge such as the characteristic "choo-choo" sound the engine emits (ref. 2) when encountering this condition. Thirty-three hours were accumulated on the engine during conduct of the UETP test conditions and the repeat run, condition 6A. Also, the recommended warmup time of 5 minutes at military power before testing and recommended cooldown time before shutdown were observed.

Representative data from conditions 6 and 6A (Table I) are shown in figures 23(a) to 23(d) These are plots originally recommended by the Working Group and incorporated into the General Test Plan (ref. 1) except that either corrected high or low rotor speed was substituted for engine pressure ratio because speed appeared to be much more representative independent parameter. The results of the comparison are presented herein.

Deterioration was evaluated through the use of a least squares curves fit applied to each set of data in figures 23(a) to 23(d). The quadratic equation resulting from each curve fit was then used to calculate the dependent variable at either the target value of corrected high rotor speed of 8900 rpm or the corresponding corrected low rotor speed (the low rotor speed being determined from a speed ratio vs corrected high rotor speed plot). Corrected fuel flow, corrected airflow, and compressor pressure and temperature ratios all show less than a 0.1% change from the first condition, 6, to the last test condition, 6A. The speed ratio, NLQNH, and corrected SFC variation were less than 0.2% but engine temperature and pressure ratio changed by more than 1% while corrected net thrust increased by 0.75%. The large engine temperature and pressure ratio changes are due to the rotation of the tailpipe, mentioned in section 3.2.1, which altered the position of the nozzle inlet plane, station 7, rakes.

4.2.2 Engine 2, S/N 615037

4.2.2.1 Airflow, Net Thrust, and Specific Fuel Consumption

The trends, but not the magnitudes, in all the data plots for engine 2, shown in figures 24 to 32, are similar to

those presented for engine 1. Thus, the discussion of the data will be limited to the differences in the two sets of data. Inlet temperature variation and its influence on airflow, net thrust and specific fuel consumption were investigated in test conditions 1, 2, 3, and 4 (see Table I). It should be noted that condition 3, not run for engine 1, was run for this engine.

Even though attempts were made to prevent exhaust gas recirculation through the test cell bypass line, these gases still reached the engine inlet as described above in section 4.2.1. The temperature distortion levels at the engine inlet, however, were less than for the first engine tests.

If the data from condition 3 are removed from figure 24, a plot of corrected airflow ratio against inlet temperature, the trend for engine 2 is indeed similar to the trend shown for engine 1 in figure 13 but different in magnitude.

Figure 26 shows a change in corrected airflow ratio with ram pressure ratio at the two lowest ram pressure ratios, a trend not shown for engine 1 in figure 16. An investigation into the cause of this difference revealed that the exhaust nozzle pressure ratio for the two lowest conditions in figure 26 was 1.89 and 2.01, respectively, while all other data including that for engine 1 were at an exhaust nozzle pressure ratio of 2.04 or greater. From this it was concluded that the exhaust nozzle was most likely not choked for the two conditions in question.

As with the corrected airflow ratio against inlet temperature plot, removal of condition 3 from the corrected net thrust plot shown in figure 27 resulted in similar curves but of different magnitudes from engine 1 results.

Figures 29 and 32, which show corrected net thrust ratio and SFC ratio against ram pressure ratio, would show a much better fit if a higher order least squares quadratic curve fit were used. However, for consistency with all the other plots this was not done. Also, removal of condition 3 from both figures would show that the trends of these two plots would be similar to those shown for engine 1.

4.2.2.2 Engine and Component Deterioration

To document engine and component deterioration, NASA ran the identical condition as the first and last test conditions (i.e., condition 6 in Table I). Before making comparisons, it should be noted that approximately 3-1/2 hours were accumulated on the engine between the time it was received and the first time condition 6 was run. This time was devoted to trimming the engine for Jet A fuel and conducting facility calibration tests. This involved a

number of excussions from idle to military power and return using slow throttle movements. No high vibrations were encountered during this preliminary testing nor were they encountered at any other time during conduct of the UETP test conditions.

Approximately 22 hours were accumulated on the engine during conduct of the UETP test conditions specified in Table I before the repeat run of condition 6. No stalls were indicated by the high response instrumentation used as stall detectors nor were there any audible indications of stall. The maximum turbine discharge temperature, T5, was kept at or below 883 K except for one excursion when the temperature, for a brief instant, reached 903 K because of an overshoot during an acceleration to military power. At this temperature, an automatic facility limiting device caused a "chop" to idle. This temperature of 903 K was still well below the maximum allowable temperature of 933 K so no further action was taken or required. This was also the only instance in which anything other than a slow throttle movement occurred. The recommended warmup time at military power before testing and cooldown time before shutdown were also observed.

Representative data from the repeat runs of condition 6 (referred to as 6 and 6A in Table I) are shown in figures 33(a) to 33(d). These data were evaluated using a least squares curve fit to determine deterioration. The quadratic equation resulting from each curve fit was used to calculate the dependent variable at the target value or at the corresponding corrected low rotor speed - the low rotor speed being determined from a speed ratio, NLQNH, vs corrected high rotor speed, NHR plot. The compressor temperature ratio, corrected fuel flow and corrected airflow showed a 0.1% or less change, the low rotor to high rotor speed ratio and engine pressure ratio, P7Q2, and corrected SFC showed less than a 0.2% change and the compressor pressure ratio showed less than a 0.3% change. Engine temperature ratio, T7Q2 and corrected net thrust changed by approximately 0.44%.

5.0 FINAL DATA PACKAGE

A summary of test results for both engines with performance normalized to SLS conditions and desired setting conditions is presented in Table IV. As mentioned in section 3.3, test data will be transmitted, upon request, on magnetic tapes supplied by the requesting facility after the Working Group Chairman has approved their release.

6.0 CONCLUDING REMARKS

As part of the AGARD Uniform Engine Testing Program, NASA Lewis Research Center tested two J57-19W turbojet engines in an altitude test facility at conditions specified by the AGARD Propulsion and Energetics Panel,

Working Group 15, using common test hardware, instrumentation and data acquisition and reduction procedures. Some observations concerning the NASA involvement in the engine testing, particularly with regard to engine performance, data scatter, and other items which influenced the test data, are presented herein.

The engines performed satisfactorily as there were no unusual occurrences which affected the quality of the test data. Also, engine deterioration, monitored by the common instrumentation, was well within the estimated measurement uncertainties.

As expected, data scatter was minimized because of the Working Group's choice of engine type (i.e., a turbojet with no variable geometry) and test procedures. This produced the desired effect of emphasizing the influence of the individual facility's techniques on data scatter.

Some setbacks did occur which are worthy of note because the nozzle inlet and the engine inlet measurements were affected by them. The nozzle inlet temperature and pressure measurements were influenced by flow nonuniformities off the turbine exit struts. Also, an inherent facility problem of inlet temperature distortion at ram pressure ratios below 1.1 surfaced and could not be completely eliminated.

In spite of these problems, the first step has been taken in acquiring these data toward meeting the objectives of the AGARD Uniform Engine Testing Program. Test data are ready for transmittal to interested parties after the Working Group Chairman has approved their release.

APPENDIX A

MODIFIED TAILPIPE - NOZZLE CALIBRATION

Following from the fact that the tailcone on the J57 engine extended through the nozzle exit plane (see fig. 2), this configuration was modified by replacing this nozzle (referred to as the Bill of Material or BOM nozzle) with a cylindrical tailpipe and convergent nozzle (see figure 3 for a photograh of the two nozzles). This necessitated a calibration test sequence with the new tailpipe-nozzle assembly. The procedure for this calibration was as follows:

1. The engine was operated in BOM configuration to gather the appropriate performance match parameters (i.e., EPR, NL, T5, and NH).

2. The BOM nozzle was removed and the modified tailpipe-nozzle assembly was installed. The nozzle exit area was less than that calculated to produce equivalence of the match parameters with the BOM configuration.

3. The engine was operated with the modified configuration and match parameter data collected.

4. The nozzle exit area was cut slightly smaller than the estimated final area.

5. Step 3 was repeated.

6. A final nozzle exit area cut was made based on data from steps 3 and 5 (e.g., EPR vs NH) and the engine operated to verify the match with the BOM configuration.

APPENDIX B

CALCULATION OF NET THRUST

Net thrust was calculated from engine gross thrust, FG, and a ram drag term, WA1*V0. This discussion will center on how the gross thrust term was determined in the NASA LeRC altitude facilities because the ram drag term involves a relatively straightforward calculation.

The summation of forces was equal to the difference between the engine exit momentum, W8*V8, and the engine inlet momentum, WA1*V1, using the conservation of momentum principle. Since the engine testing was done in an altitude test facility, pressure-area terms and test installation calibration factors were considered. In equation form and using the terminology of the following figure with pressures referenced to cell pressure, PAMB, this leads to:

$$FMEAS + A1(PS1 - PAMB) - A8(PS8 - PAMB) + \int_{A1}^{A8} (P - PAMB)dA$$

$$- FSTAND = W8*V8 - WA1*V1$$

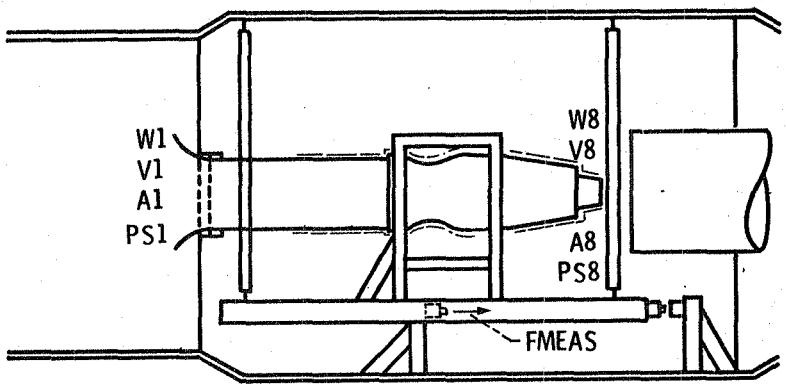

Basic thrust nomenclature.

Engine gross thrust was defined as follows:

$$FG = W8*V8 + A8(PS8 - PAMB)$$

Therefore,

$$FG = FMEAS + WA1*V1 + A1(PS1 - PAMB) + \int_{A1}^{A8} (P - PAMB)dA + FSTAND$$

The stand term, FSTAND, involved those forces on the thrust stand when loads were applied and another term related to the friction forces caused by flow through the labyrinth seal and by cell cooling air, should it impinge on the engine.

Since net thrust was defined as

FN = FG - WA1*VO

This results in

$$FN = FMEAS + WA1*V1 + A1(PS1 - PAMB) + \int_{A1}^{A8} (P - PAMB)dA + FSTAND - WA1*VO$$

APPENDIX C

CALCULATION OF INLET TOTAL AIRFLOW

The method used in the altitude test facilities at NASA to calculate inlet total airflow at the airflow station, station 1, (see fig. 4 for station locations) involved the intergration of a flow per unit area calculated for each total pressure probe. The highlights of this method are presented below.

At station 1, four boundary layer rakes with eight immersions were used to measure total pressure. The immersions, as shown in the following sketch, were labeled from r_8 at the wall to r_0 in the free stream:

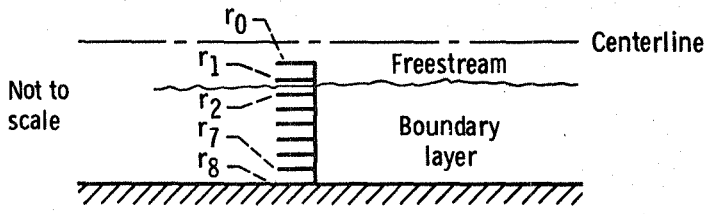

Dividing station 1 into rings, one for each probe radius, the integral

$$\int \frac{W}{A}\, dA$$

was evaluated for each ring where

$$\frac{W}{A} = \frac{PS}{\sqrt{RT}} \sqrt{\frac{2\gamma}{\gamma - 1}\left[\left(\frac{P}{PS}\right)^{(\gamma-1)/\gamma} - 1\right]\left(\frac{P}{PS}\right)^{(\gamma-1)/\gamma}}$$

Total pressure, P, was a function of radius and it was assumed that the temperature, T, static pressure, PS, and air properties, R and γ, were constant. The first assumption in this approach was that no heat transfer occurred between the plenum, where the inlet total temperature was measured, and station 1. The next assumption was that the static pressure profile across the duct at station 1 was constant - an assumption which was checked through surveys made during preliminary NASA tests. The results of these surveys and the subsequent action taken are summarized in section 3.2.2.

APPENDIX D

CALCULATION OF SFC

The ingredients of the SFC calculation, net thrust and fuel mass flow, are described in Appendix B and below, respectively. The calculation of fuel flow rate at NASA involved the use of turbine type flow meters, thermocouples and analyses of fuel samples. Two low range and two high range facility flow meters were employed while each engine was assigned its own flow meter. Both facility and engine mounted turbine meters measured volume flow but the output of the facility meters was used in the SFC calculation. Fuel mass flow was calculated from the volume flow and fuel density which, in turn, required the fuel temperature measurements and the analyses of fuel samples from each test run* to determine fuel specific gravity. The engine mounted fuel flow meters for the first engine were calibrated by Pratt & Whitney using PMC 9041 as the calibration fluid and by NASA using water as the calibration fluid. The fuel flow meters for the second engine were calibrated by NASA.

*These fuel samples are available for analysis by the Canadian Fuel Laboratories.

APPENDIX E

MEASUREMENT UNCERTAINTIES

Comments pertinent to the estimate of the measurement uncertainties for inlet total airflow, net thrust and specific fuel consumption as determined at NASA using reference 7 are presented herein, individual elemental errors are presented in Table II and the actual uncertainty estimates are presented in Table III.

Measurement Uncertainty

E-1 Airflow

Total airflow at the engine inlet was calculated at station 1 using the equation presented in Appendix C. That equation can be rewritten as follows:

$$WA1 = \frac{\pi}{4} * D1^2 * CD1 * \frac{P1}{\sqrt{T1}} \left(\frac{PS1}{P1}\right)^{1/\gamma} \sqrt{\frac{2\gamma}{R(\gamma-1)} \left[1 - \left(\frac{PS1}{P1}\right)^{(\gamma-1)/\gamma}\right]}$$

in this form, the airflow equation is the same as that shown in reference 7, equation (IV-3), except that the thermal expansion factor, F_a, molecular weight, M, and compressibility factor, z, were not included because errors associated with these values were assumed negligible. Further, the errors associated with π and γ were assumed negligible. A flow coefficient CD1 was included because it was required for the NASA airflow measurement technique as described in section 3.2.2.

The techniques described in section 6.2.1.1 of reference 7 were applied to UETP test conditions. In the above equation for airflow rate, P1 and PS1 are assumed in reference 7 to be independent measurements on two different transducers. However, following from the fact that in the NASA application P1 and PS1 were both measured on the same multiplexed (Scanivalve) transducer, it was assumed for the uncertainty estimates that the PS1 measurement was more closely represented by a differential pressure measurement (i.e., PS1 = P1 - DP). The appropriate equations for this approach are also shown in reference 7, section 6.2.1.1.

The bias error for this differential pressure, B_{DP} was estimated to be 0.013 while the precision error was estimated to be 0.009.

E-2 Net Thrust

Net thrust was calculated using the equation derived in Appendix B. The equation used for measurement uncertainty analysis for net thrust, however, was simplified in the following manner:

1. Scale force, FS, included the thrust load cell measurements, FMEAS, and the stand term, FSTAND.

2. The pressure-area term along the outer surfaces

$$\int_{A1}^{A8} (P - PAMB)dA$$

was considered negligible.

Therefore,

$$FN = WA1(V1 - V0) + A1(PS1 - PAMB) + FS$$

This is also the form of the net thrust equation found in reference 7, section 7.3. The techniques presented in section 7.3 were used to determine net thrust measurement uncertainty except that it was assumed, as stated in section E-1 above, that the PS1 measurement was more closely represented by a differential pressure measurement.

E-3 Specific Fuel Consumption

The techniques presented in reference 7, section 7.4, were used to determine specific fuel consumption, SFC, measurement uncertainty.

REFERENCES

1. UETP General Test Plan, January 1982.

2. Technical Manual, Overhaul Instructions: (USAF) T.O. 2J-J57-13.

3. Technical Manual, Illustrated Parts Breakdown: (USAF) T.O. 2J-J57-14.

4. Gas Turbine Engine Performance Station Identification and Nomenclature, SAE APR 755A.

5 Dean, G.W.: Test Procedures for Establishing the Altitude Performance of Turbofan Engines to Validate Contractual Guarantees. ASME Paper 78-GT-42, April 1978.

6. Gordon, S.; and McBride, B.: Computer Program for Calculation of Complex Chemical Equilibrium Compositions, Rocket Performance, Incident and Reflected Shocks, and Chapman-Jouguet Detonations. NASA SP-273, 1971.

7. Abernethy, R.B.; and Thompson, J.W., Jr.: Handbook Uncertainty in Gas Turbine Measurements. AEDC-TR-73-5, 1973.

TABLE I. - TEST CONDITIONS

Test	Average inlet total pressure, P		Ram ratio	Inlet total temperature, T, K	High compressor speed, NH
	psia	kPa			
1	12.0	82.7	1.00**	253	Nine throttle settings as illustrated in Section 3.1.2.2 and listed in Table III of reference 1.
2	12.0	82.7	1.00**	268	
3	12.0	82.7	1.00**	288	
4	12.0	82.7	1.00**	308	
5	12.0	82.7	1.06**	288	
6*	12.0	82.7	1.30	288	
6A*	12.0	82.7	1.30	288	
7	7.5	51.7	1.30	288	
8	5.0	34.5	1.30	288	
9	3.0	20.7	1.30	288	
10	12.0	82.7	1.70	288	

*The first condition run in the test series, 6, was repeated at the end of the test program, 6A, to evaluate engine deterioration or variation.

**NASA did accomplish the first four test points at a ram ratio of 1.00 (except condition 3 was run only for the second engine) and also did test condition 5.

TABLE II. - IDENTIFICATION OF ELEMENTAL ERROR SOURCES

Parameter - Temperature
Measurement range - 250 to 310 K

	ERROR SOURCE	PRECISION INDEX		BIAS LIMIT
		Unit of measure	Degree of freedom	Unit of measure
I	Calibration	0*	0	B_{CAL} = ±0.19 K
II	Data acquisition	-	-	B_{DA} = ±0.48 K
III	Data reduction	$S_{DA,DR}$ = 0.08 K	76	B_{DR} = ±0.15 K
		S_T = ±0.08 K	d_f = 76	B_T = ±0.54 K

Parameter - Pressure
Measurement range - 0 to 103.42 kPa

	ERROR SOURCE	PRECISION INDEX		BIAS LIMIT
		Unit of measure	Degree of freedom	Unit of measure
I	Calibration	0*	0	B_{CAL} = ±0.062 kPa
II	Data acquisition & data reduction	$S_{DA,DR}$ ±0.05% at 58.7 kPa ±0.09% at 30.5 kPa ±0.12% at 13.9 kPa	34	$B_{DA,DR}$ ±0.01% at 58.7 kPa ±0.06% at 30.5 kPa ±0.13% at 13.9 kPa
		$S_T = S_{DA,DR}$	d_f = 34	B_T ±0.11% at 58.7 kPa ±0.23% at 30.5 kPa ±0.47% at 13.9 kPa

*All calibration errors were considered bias errors.

TABLE II. - IDENTIFICATION OF ELEMENTAL ERROR SOURCES (Concluded)

Parameter - Scale Force
Measurement Range - 0 to 44.5 kN

	ERROR SOURCE	PRECISION INDEX			BIAS LIMIT
		Unit of measure		Degree of freedom	Unit of measure
I	Calibration	0*		0	B_{CAL} = ±32.0 N
II	Data Acquisition	$S_{DA,DR}$	31.5 N + 0.36% Rdg at 3.9 kN		B_{DA} = ±19.6 N
III	Data Reduction		31.5 N + 0.14% Rdg at 22.2 kN		B_{DR} = ±22.2 N
			31.5 N + 0.06% Rdg at 35.6 kN		
		$S_T = S_{DA,DR}$		$d_f > 30$	B_T = ±43.6 N

Parameter - Fuel Flow
Measurement Range - 0 to 1260 g/sec

	ERROR SOURCE	PRECISION INDEX			BIAS LIMIT
		Unit of measure		Degree of freedom	Unit of measure
I	Calibration	0*		0	B_{CAL} = ±0.29% Rdg
II	Data Acquisition & Data Reduction	$S_{DA,DR}$	0.48% Rdg at 0.63 kg/sec	-	$B_{DA,DR}$ = ±0.14%
Rdg			(eng. 1) 0.62% Rdg at 0.315 kg/sec		
			0.20% Rdg at 0.63 kg/sec		
			(eng. 2) 0.35% Rdg at 0.315 kg/sec		
		$S_T = S_{DA,DR}$		$d_f > 30$	B_T = ±0.32% Rdg

*All calibration errors were considered bias errors.

TABLE III - ESTIMATED PERFORMANCE PARAMETER UNCERTAINTIES

(a) Engine: S/N 607594

Cond.	Rdg.	P2, kPa	T2, K	Ram ratio	NHR, rpm	Airflow				Net thrust				SFC			
						Precision, S, %	Degrees of freedom	Bias, B, %	Uncertainty, U, %	Precision, S, %	Degrees of freedom	Bias, B, %	Uncertainty, U, %	Precision, S, %	Degrees of freedom	Bias, B, %	Uncertainty, U, %
1	370	82.8	255	1.00	8842	0.24	> 30	0.39	0.9	0.30	> 30	0.31	0.9	0.60	> 30	0.45	1.7
2	345	83.3	269	1.01	8846	0.21	> 30	0.38	0.8	0.26	> 30	0.26	0.8	0.58	> 30	0.41	1.6
4	320	82.9	310	1.00	8896	0.22	> 30	0.36	0.8	0.34	> 30	0.32	1.0	0.58	> 30	0.46	1.6
5	211	82.9	289	1.07	8854	0.23	> 30	0.37	0.8	0.21	> 30	0.21	0.6	0.52	> 30	0.38	1.4
6	174	83.0	287	1.31	8890	0.15	> 30	0.36	0.7	0.22	> 30	0.22	0.7	0.54	> 30	0.39	1.5
7	295	51.8	287	1.29	8916	0.31	> 30	0.51	1.1	0.34	> 30	0.34	1.0	0.68	> 30	0.47	1.8
8	275	34.6	288	1.28	8935	0.37	> 30	0.73	1.5	0.49	> 30	0.49	1.5	0.79	> 30	0.58	2.2
9	250	20.6	289	1.30	8938	0.78	> 30	1.29	2.9	0.76	> 30	0.80	2.3	0.79	> 30	0.86	2.4
10	192	83.3	287	1.68	8880	0.20	> 30	0.36	0.8	0.24	> 30	0.26	0.7	0.55	> 30	0.41	1.5

(b) Engine: S/N 615037

1	678	83.1	256	1.01	8853	0.22	> 30	0.40	0.8	0.29	> 30	0.29	0.9	0.38	> 30	0.43	1.2
2	654	83.5	270	1.00	8949	0.20	> 30	0.36	0.8	0.34	> 30	0.29	1.0	0.40	> 30	0.43	1.2
3	755	83.2	291	1.00	8838	0.23	> 30	0.40	0.9	0.39	> 30	0.38	1.2	0.46	> 30	0.49	1.4
4	728	83.1	309	1.00	8650	0.28	> 30	0.47	1.0	0.41	> 30	0.40	1.2	0.49	> 30	0.51	1.5
5	783	83.0	290	1.07	8832	0.23	> 30	0.40	0.9	0.22	> 30	0.22	0.7	0.33	> 30	0.39	1.0
6	565	83.0	288	1.30	8876	0.21	> 30	0.37	0.8	0.23	> 30	0.24	0.7	0.32	> 30	0.40	1.0
7	696	51.7	288	1.30	8922	0.33	> 30	0.53	1.2	0.36	> 30	0.36	1.1	0.48	> 30	0.48	1.4
8	621	34.5	288	1.29	8926	0.51	> 30	0.78	1.8	0.52	> 30	0.52	1.6	0.64	> 30	0.61	1.9
9	615	20.7	287	1.30	8992	0.86	> 30	1.27	3.0	0.75	> 30	0.80	2.3	0.86	> 30	0.86	2.6
10	583	83.1	289	1.71	8855	0.21	> 30	0.38	0.8	0.26	> 30	0.29	0.8	0.35	> 30	0.43	1.1

TABLE IV - UNIFORM ENGINE TESTING PROGRAM

SUMMARY OF TEST RESULTS

(a) ENGINE S/N 607594

Test	Desired setting condition			Performance Normalized to Sea Level Static Conditions									Speed ratio, NLQNH
	P2AV, kPa	T2AV, K	P2QAMB	NLR, rpm	NHR, rpm	WA1R, kg/s	WFR, g/s	FGR, kN	FSLS, kN	FNR, kN	SFCR, g/kN-s	SFCSLS, g/kN-s	
1	82.7	253	1.0	5373	8900	65.2	736	32.9	32.9	32.9	22.4	22.4	0.604
2	82.7	268	1.0	5381	8900	65.3	746	33.2	33.2	33.2	22.5	22.5	0.605
3	82.7	288	1.0	-	8900	-	-	-	-	-	-	-	-
4	92.7	308	1.0	5397	8900	65.1	761	33.3	33.3	33.3	22.8	22.8	0.606
5	82.7	288	1.06	5409	8900	65.3	749	36.6	33.1	28.1	26.7	22.6	0.608
6	82.7	288	1.3	5433	8900	65.5	747	43.1	32.9	25.1	29.7	22.7	0.610
7	51.7	288	1.3	5454	8900	65.0	774	43.3	33.2	25.5	30.3	23.3	0.613
8	34.5	288	1.3	5480	8900	64.2	812	43.5	33.4	25.9	31.2	24.2	0.616
9	20.7	288	1.3	5515	8900	62.7	885	43.8	33.8	26.6	33.2	26.1	0.620
10	82.7	288	1.7	5435	8900	65.4	745	49.2	32.8	24.1	30.8	22.7	0.611
11	101.3	288	1.0	-	8900	-	-	-	-	-	-	-	-
6A	82.7	288	1.3	5425	8900	65.3	742	42.8	32.7	24.9	29.8	22.7	0.610

Test	Desired setting condition			Performance Adjusted to Desired Setting Conditions							Station 7 Ratios		
	P2AV, kPa	T2AV, K	P2QAMB	NLRD, rpm	NHRD, rpm	WA1RD, kg/s	WFRD, g/s	FGRD, kN	FNRD, kN	SFCRD, g/kN-s	P7QAMB	P7Q2	T7Q2
1	82.7	253	1.0	5430	8675	64.1	748	35.0	35.0	21.3	1.936	2.025	2.666
2	82.7	268	1.0	5440	8775	59.8	701	32.1	32.1	21.8	1.946	2.037	2.668
3	82.7	288	1.0	-	8875	-	-	-	-	-	-	-	-
4	92.7	308	1.0	5434	9075	49.2	581	24.6	24.6	23.6	1.952	2.036	2.664
5	82.7	288	1.06	5441	8875	53.9	626	28.8	23.5	26.6	2.037	2.027	2.660
6	82.7	288	1.3	5474	8875	54.2	630	32.3	21.3	29.6	2.462	2.023	2.649
7	51.7	288	1.3	5515	8900	33.8	415	20.6	13.7	30.2	2.509	2.034	2.700
8	34.5	288	1.3	5431	8825	21.5	266	12.8	8.4	31.4	2.496	2.050	2.781
9	20.7	288	1.3	5421	8750	12.4	168	7.5	5.0	33.7	2.552	2.072	2.913
10	82.7	288	1.7	5468	8875	54.0	625	35.7	20.3	30.8	3.167	2.013	2.645
11	101.3	288	1.0	-	8875	-	-	-	-	-	-	-	-
6A	82.7	288	1.3	5454	8875	53.9	621	31.9	20.9	29.7	2.491	2.012	2.646

TABLE IV - Concluded

(b) ENGINE S/N 615037

Test	Desired setting condition			Performance Normalized to Sea Level Static Conditions									Speed ratio, NLQNH
	P2AV, kPa	T2AV, K	P2QAMB	NLR, rpm	NHR, rpm	WA1R, kg/s	WFR, g/s	FGR, kN	FSLS, kN	FNR, kN	SFCR, g/kN-s	SFCSLS, g/kN-s	
1	82.7	253	1.0	5304	8900	63.9	703	31.7	31.7	31.7	22.2	22.2	0.596
2	82.7	268	1.0	5311	8900	64.1	710	31.9	31.9	31.9	22.3	22.3	0.597
3	82.7	288	1.0	5302	8900	63.6	706	31.6	31.6	31.6	22.4	22.4	0.596
4	92.7	308	1.0	5309	8900	63.5	712	31.6	31.6	31.6	22.5	22.5	0.597
5	82.7	288	1.06	5319	8900	63.8	704	35.0	31.5	26.6	26.5	22.4	0.598
6	82.7	288	1.3	5363	8900	64.5	710	41.7	31.6	24.0	29.7	22.5	0.603
7	51.7	288	1.3	5387	8900	64.0	735	42.0	31.9	24.4	30.2	23.1	0.605
8	34.5	288	1.3	5414	8900	63.4	773	42.1	32.1	24.7	31.3	24.1	0.608
9	20.7	288	1.3	5443	8900	61.6	836	42.2	32.3	25.3	33.0	25.9	0.612
10	82.7	288	1.7	5369	8900	64.6	710	47.9	31.6	23.2	30.7	22.5	0.603
11	101.3	288	1.0	-	8900	-	-	-	-	-	-	-	-
6A	82.7	288	1.3	5353	8900	64.3	705	41.5	31.4	23.7	29.6	22.5	0.601

Test	Desired setting condition			Performance Adjusted to Desired Setting Conditions							Station 7 Ratios		
	P2AV, kPa	T2AV, K	P2QAMB	NLRD, rpm	NHRD, rpm	WA1RD, kg/s	WFRD, g/s	FGRD, kN	FNRD, kN	SFCRD, g/kN-s	P7QAMB	P7Q2	T7Q2
1	82.7	253	1.0	5425	8800	63.9	742	35.1	35.1	21.1	1.901	1.999	2.501
2	82.7	268	1.0	5481	8925	60.5	719	33.1	33.1	21.7	1.906	1.997	2.496
3	82.7	288	1.0	5483	9000	54.9	652	29.1	29.1	22.4	1.892	1.978	2.493
4	92.7	308	1.0	5545	9200	51.1	624	26.8	26.8	23.3	1.897	1.975	2.499
5	82.7	288	1.06	5520	9000	55.5	665	30.8	25.3	26.2	2.006	1.969	2.490
6	82.7	288	1.3	5495	9000	55.0	643	33.2	21.9	29.3	2.445	1.970	2.465
7	51.7	288	1.3	5500	8925	33.9	411	20.7	13.8	29.8	2.451	1.979	2.538
8	34.5	288	1.3	5510	8925	22.3	284	13.7	9.2	30.9	2.421	1.995	2.609
9	20.7	288	1.3	5494	8875	12.8	178	8.0	5.4	32.7	2.478	1.995	2.752
10	82.7	288	1.7	5490	9000	54.8	639	36.6	21.0	30.5	3.204	1.968	2.465
11	101.3	288	1.0	-	9000	-	-	-	-	-	-	-	-
6A	82.7	288	1.3	5520	9000	55.4	656	33.8	22.5	29.2	2.459	1.964	2.477

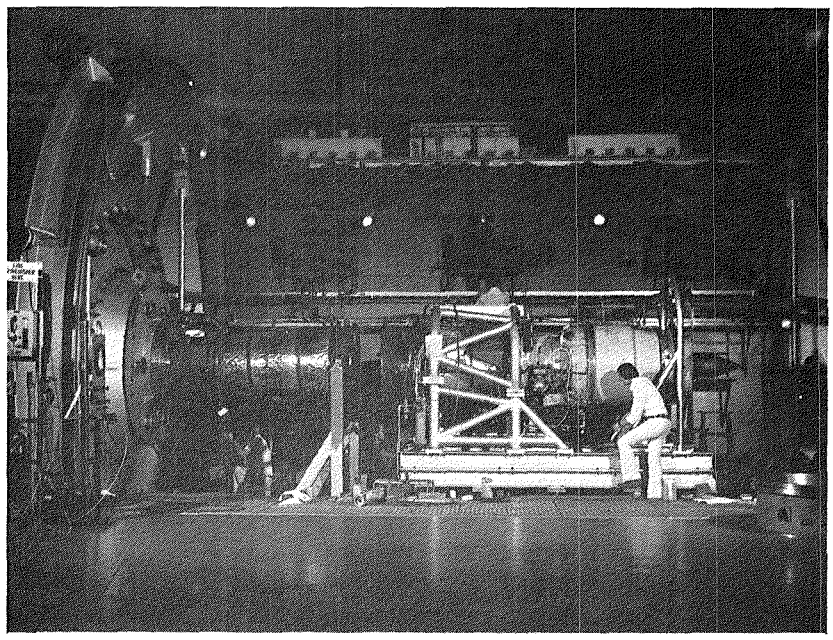

(a)

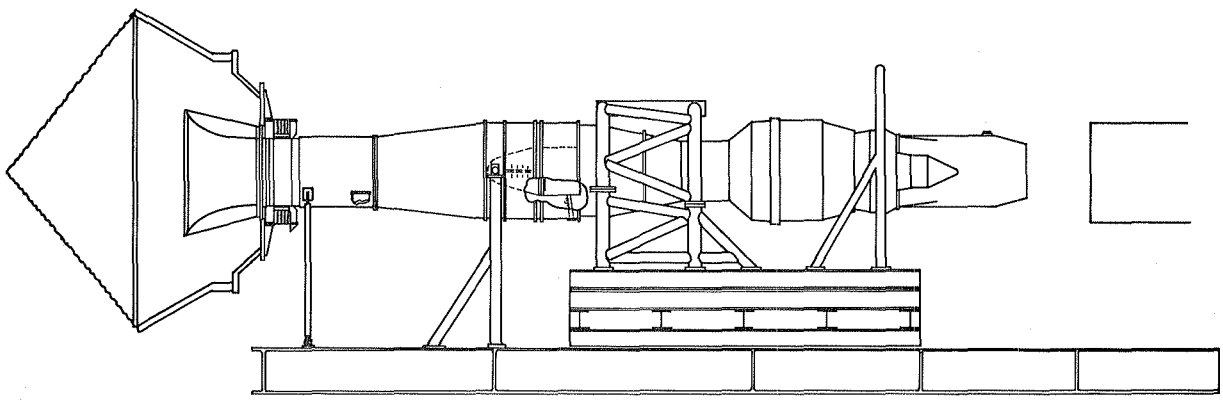

(b)

(a) J57 engine installation.
(b) Schematic of J57 engine installation.

Figure 1. - J57 engine installation in Propulsion System Laboratory test cell 3 (PSL-3).

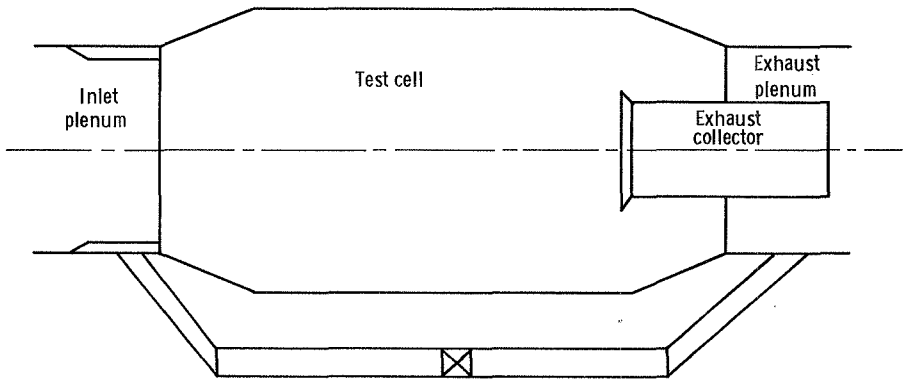

(c) Schematic of PSL-3 bypass line.

Figure 1. - Concluded.

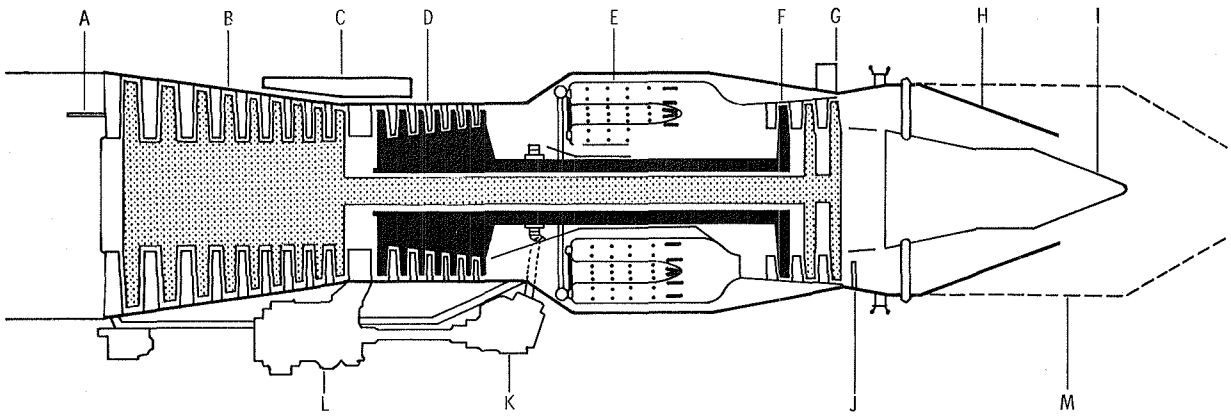

A. EPR probe (inlet pressure)
B. Low pressure compressor
C. Oil supply tank
D. High pressure compressor
E. Burner cans
F. First stage turbine
G. Second and third stage turbine
H. Nozzle
I. Tail cone
J. EPR probe (exhaust pressure)
K. Accessory drive elbow
L. Accessory drive housing
M. Modified tailpipe and nozzle assembly

Figure 2. - J57 engine schematic.

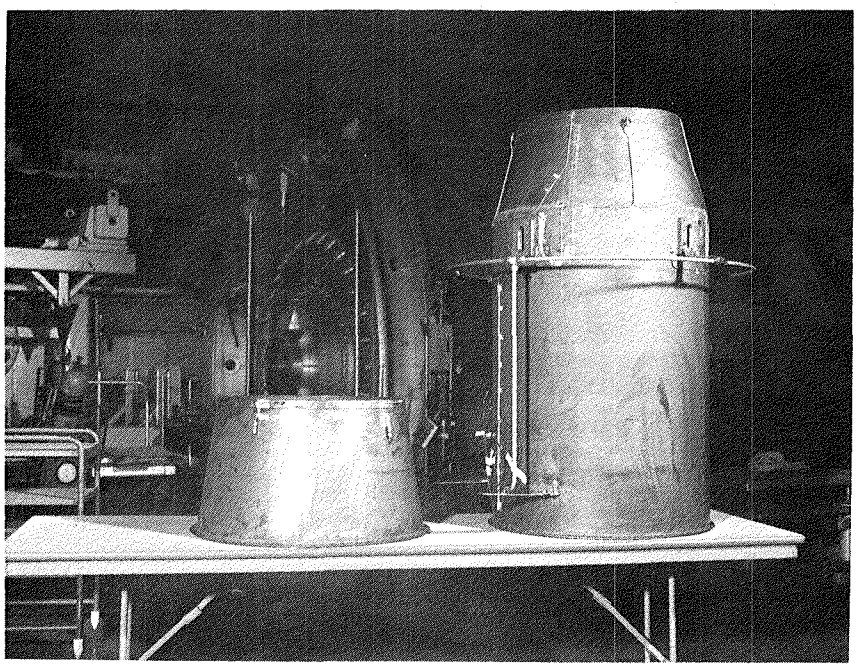

Figure 3. - BOM nozzle and tailpipe with convergent nozzle.

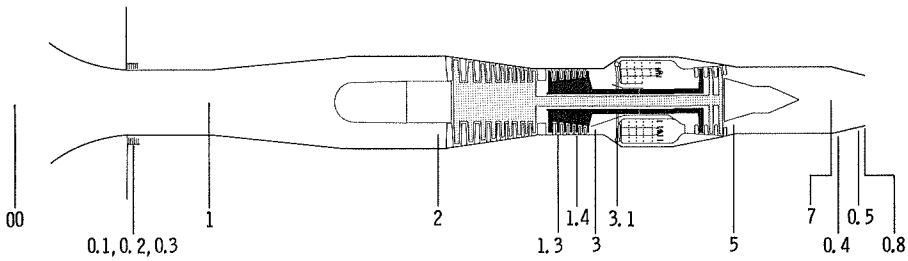

Station No.	Description
0.0	Inlet plenum
0.1, 0.2, 0.3	Labyrinth seal
1.0	Airflow station
2.0	Engine or LPC inlet
1.3	LPC bleed annulus
1.4	LPC bleed port
3.0	Combustor inlet
3.1	Combustor diffuser exit
5.0	LPT exit
7.0	Exhaust nozzle inlet
0.4, 0.5, 0.8	Exhaust nozzle (external)

Figure 4. - Instrumentation locations.

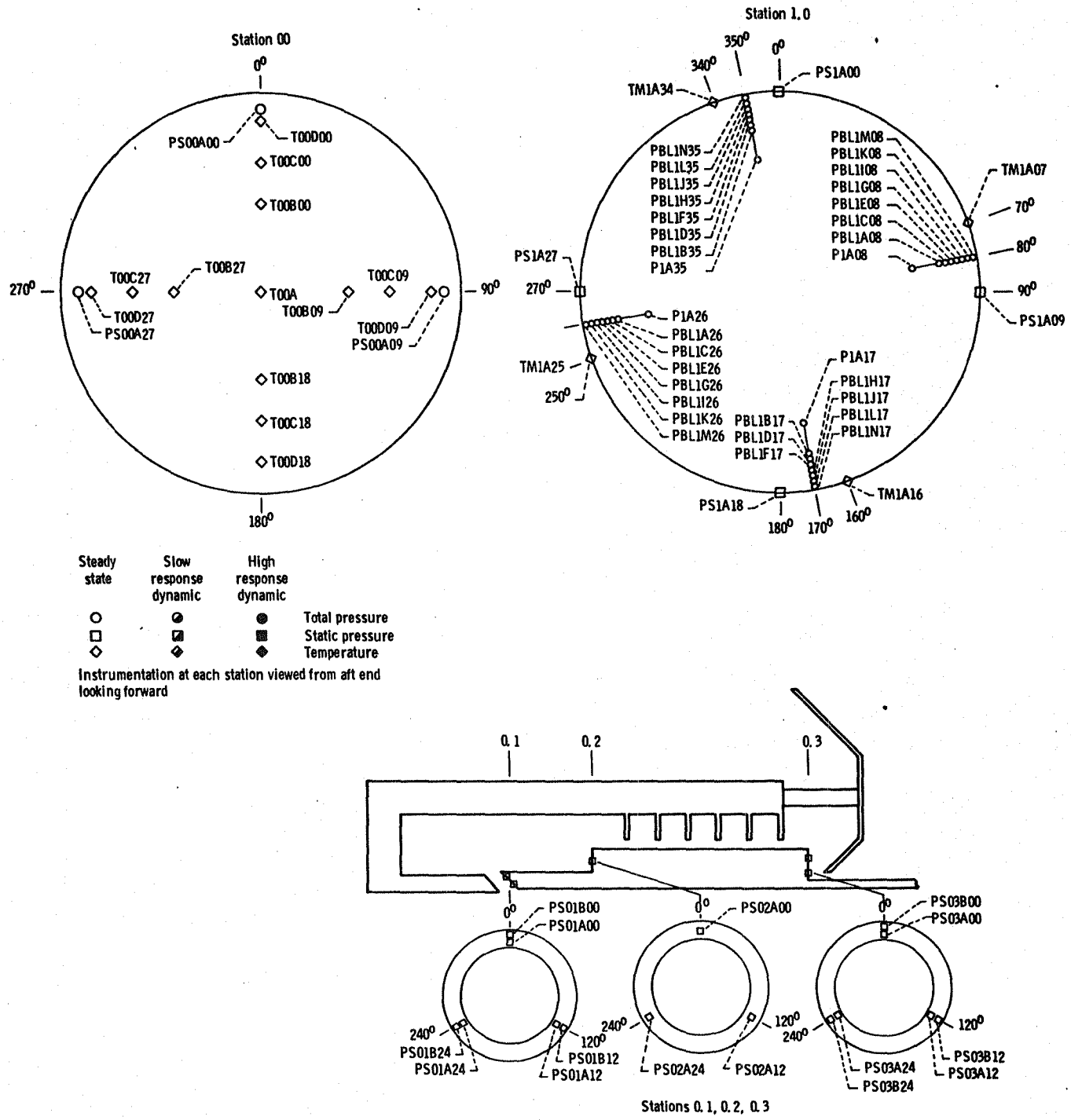

Instrumentation at each station viewed from aft end looking forward

Stations 0.1, 0.2, 0.3

Figure 4. - Continued.

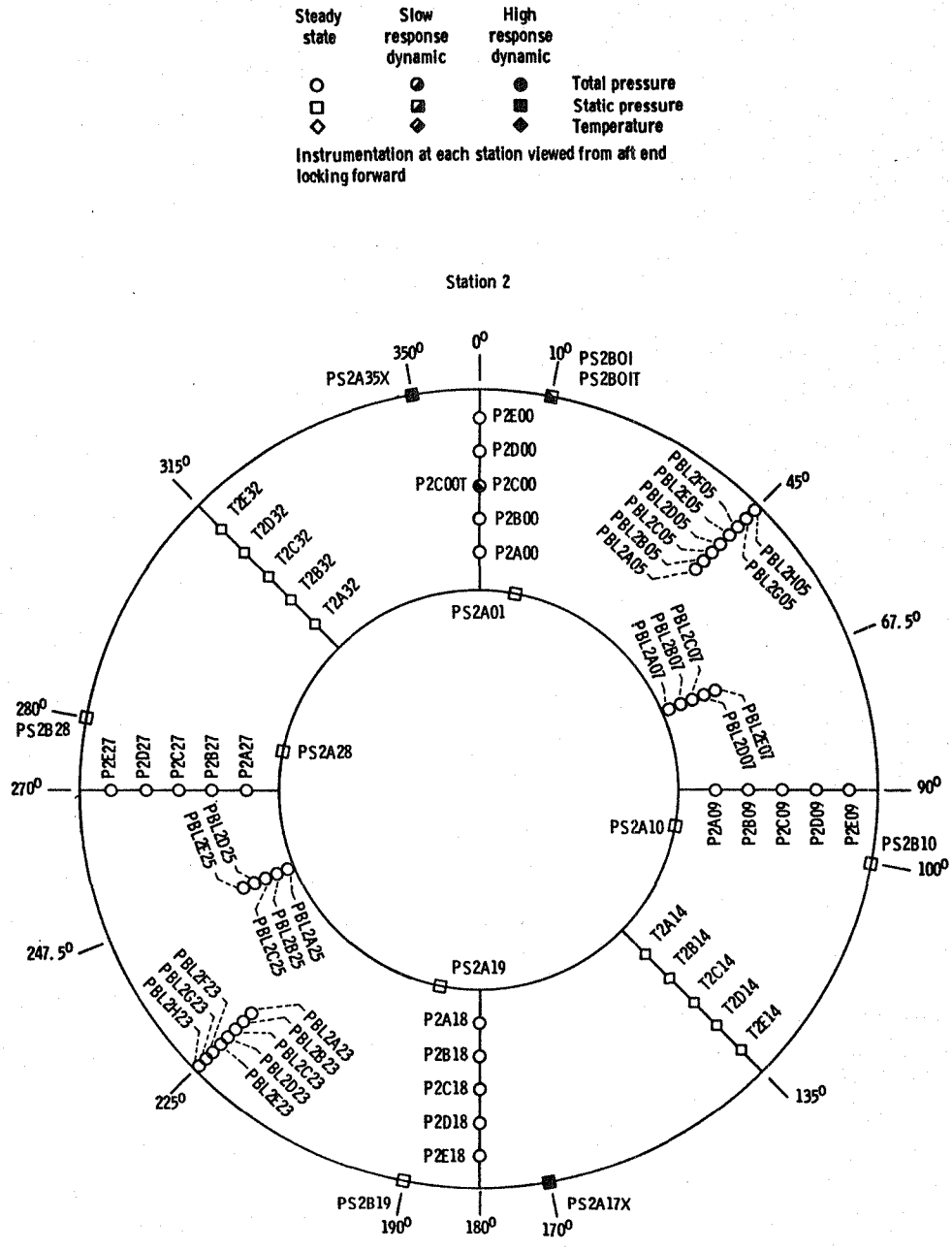

Figure 4. - Continued.

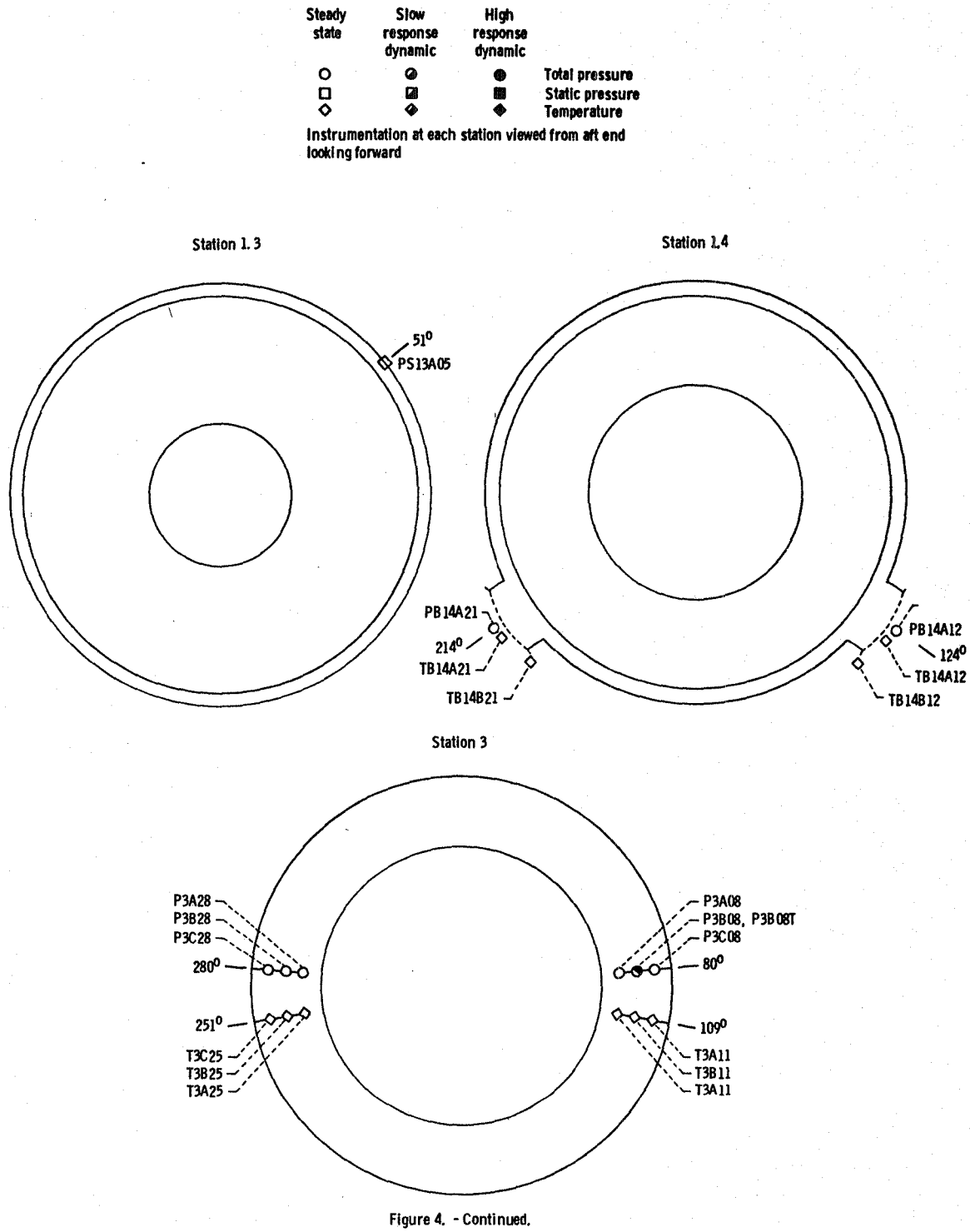

Figure 4. - Continued.

Steady state	Slow response dynamic	High response dynamic	
○	◔	●	Total pressure
□	◪	■	Static pressure
◇	◈	◆	Temperature

Instrumentation at each station viewed from aft end looking forward

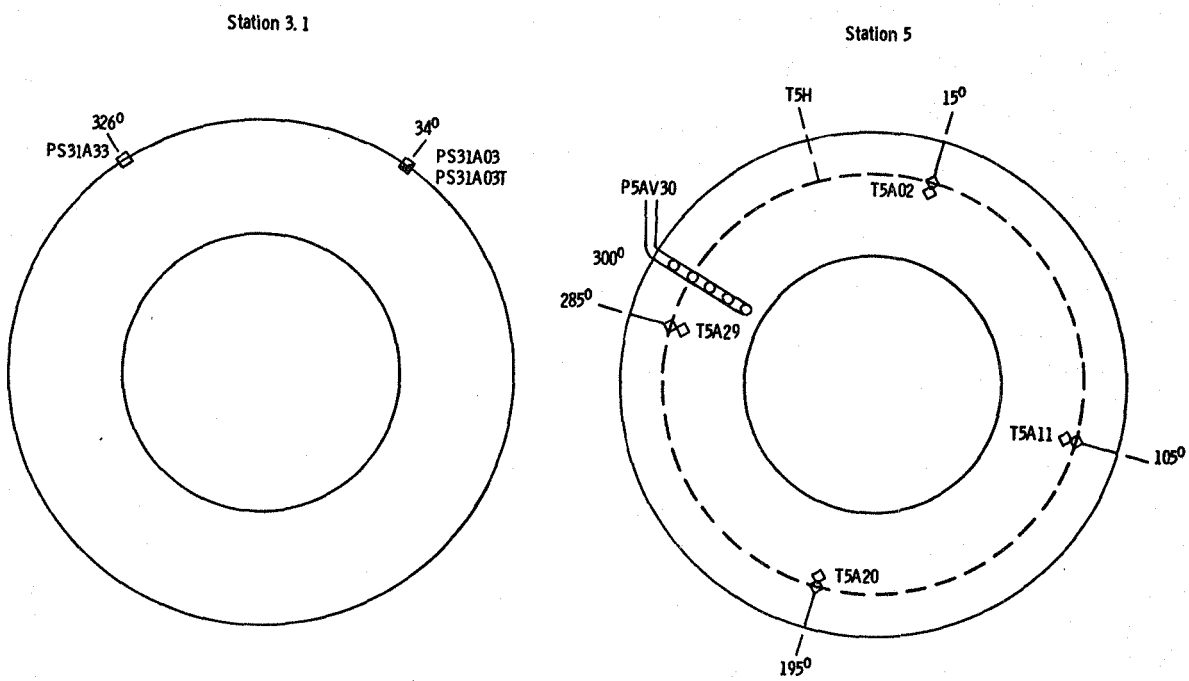

Figure 4. - Continued.

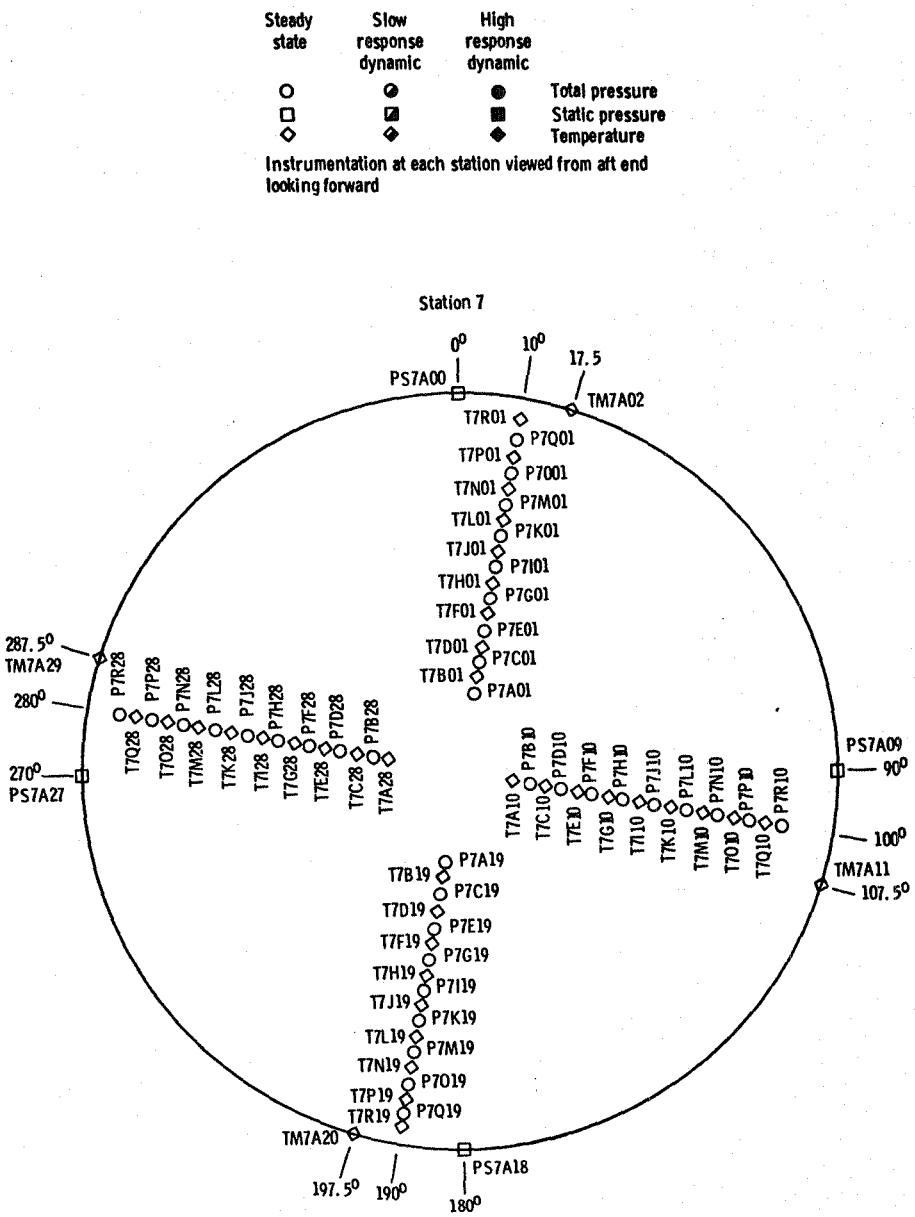

Figure 4. - Continued.

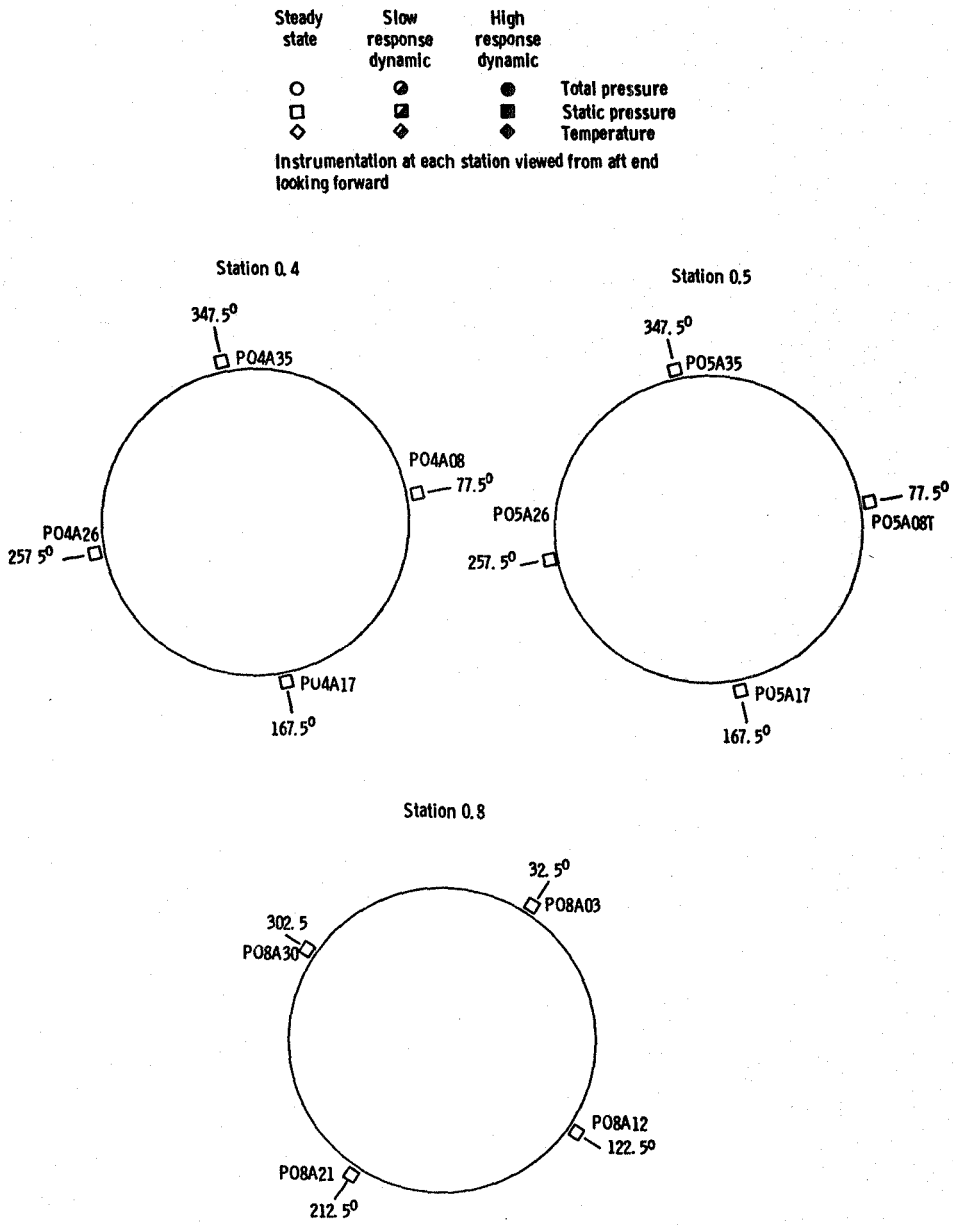

Figure 4. - Concluded.

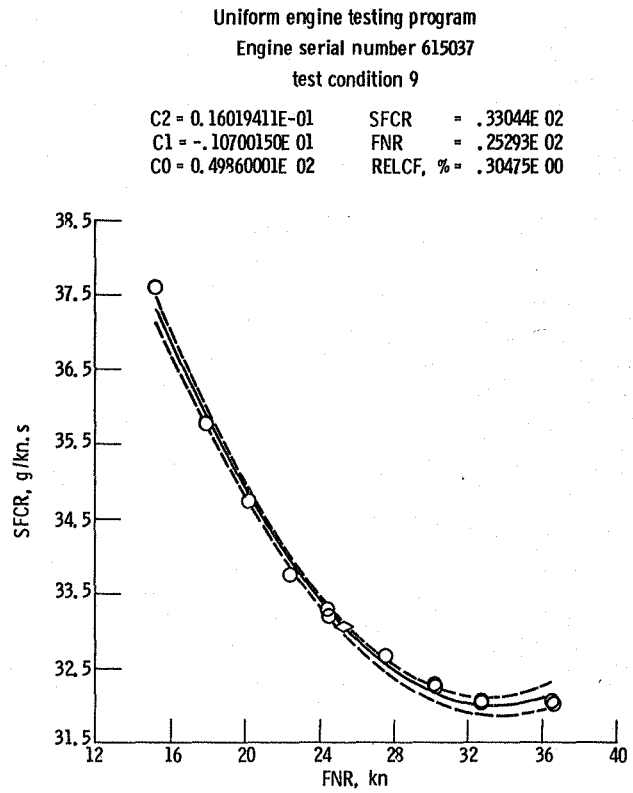

Figure 5. - Specific fuel consumption vs net thrust.

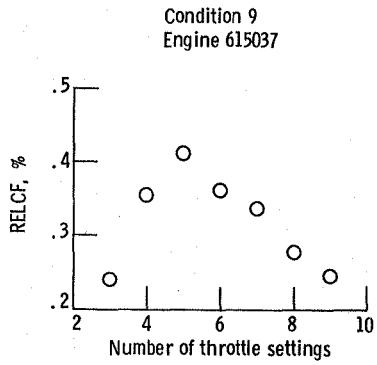

Figure 6. - Variation of random error limit of curve fit, RELCF, with the number of throttle settings.

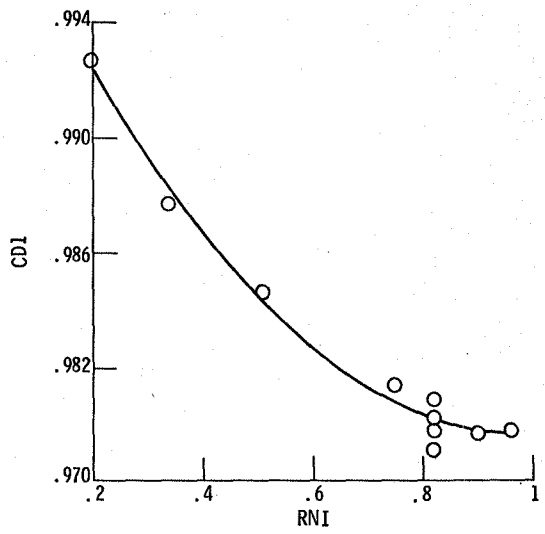

Figure 7. - Variation of the station 1 flow coefficient with Reynolds number index.

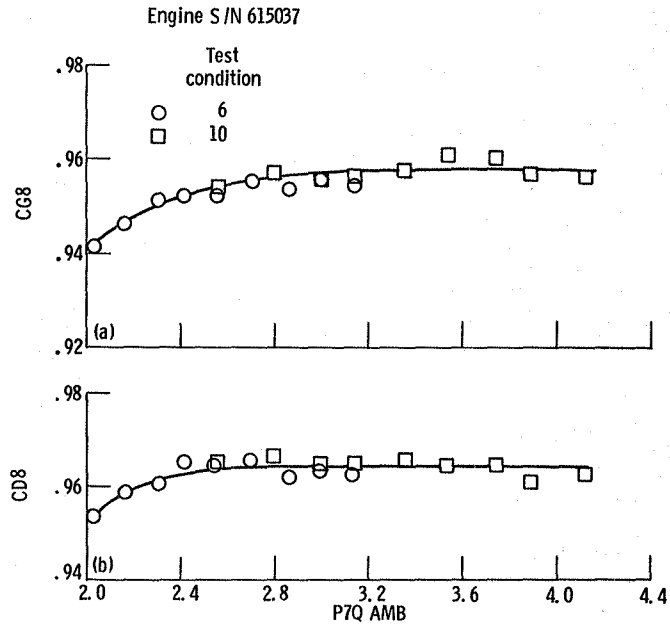

(a) Exhaust nozzle thrust coefficient.

(b) Exhaust nozzle flow coefficient.

Figure 8. - Variation of exhaust nozzle coefficients with nozzle pressure ratio.

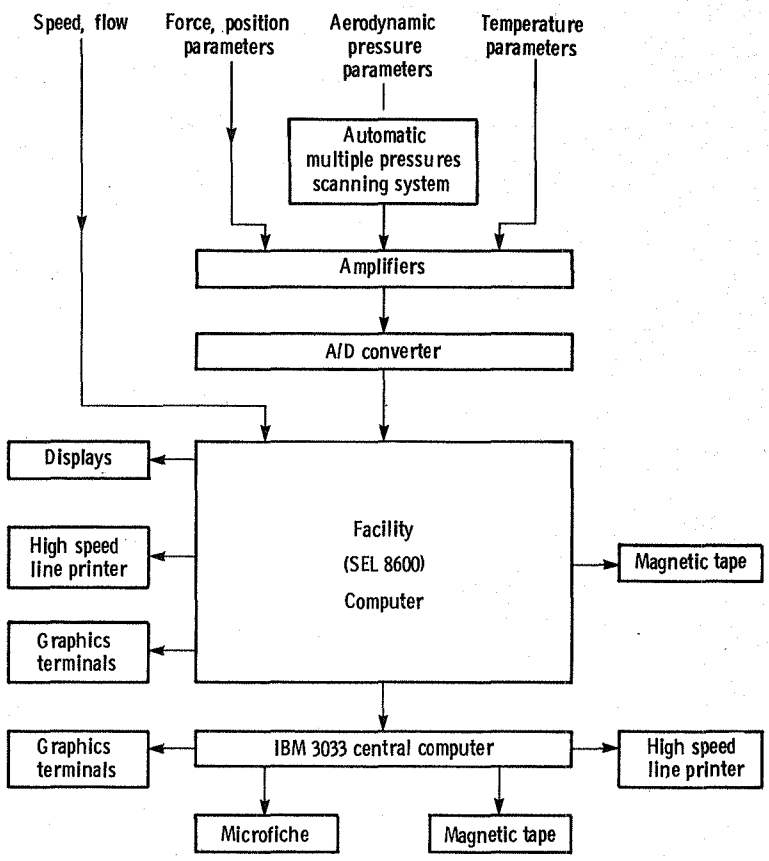

Figure 9. - Digital data acquisition system and data processing system.

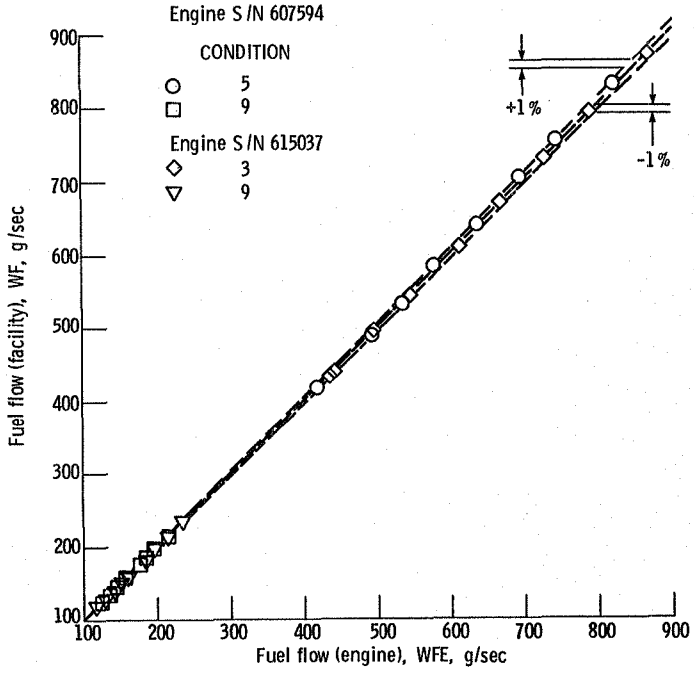

Figure 10. - Comparison of facility and engine fuel flow meters.

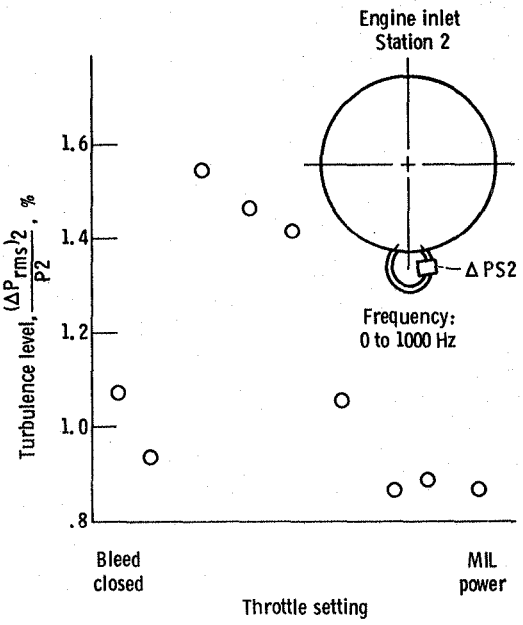

Figure 11. - Typical variation of turbulence level at engine inlet with throttle setting.

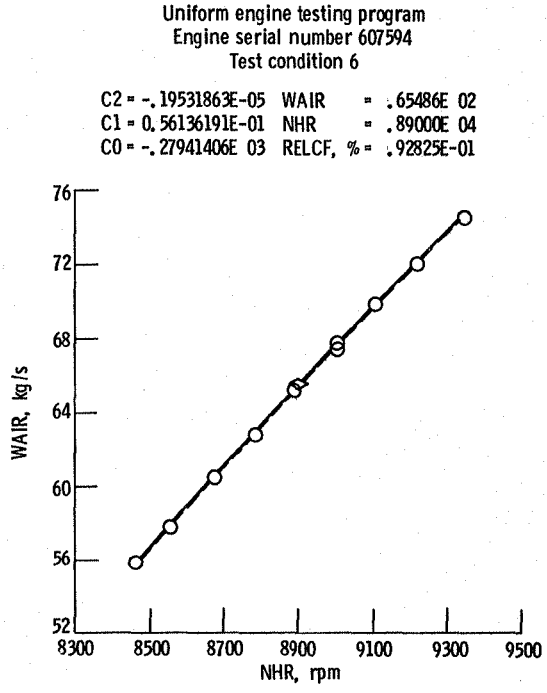

Figure 12. - Airflow vs high rotor speed.

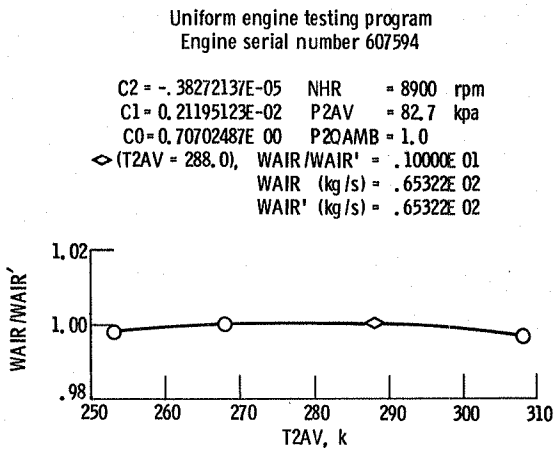

Figure 13. - Temperature influence.

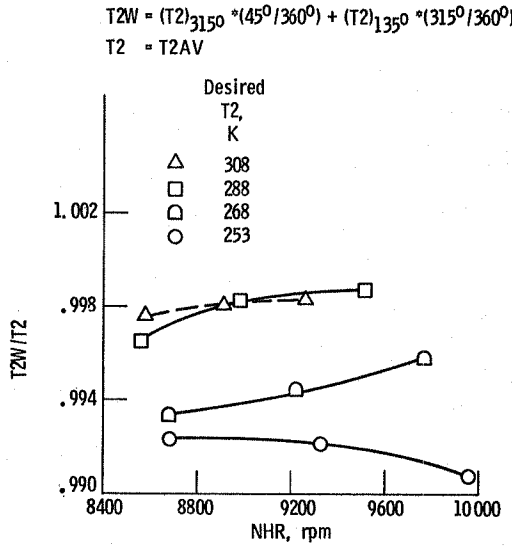

Figure 14. - Comparison of weighted and average engine inlet temperature. Ram pressure ratio = 1. 0. Engine S/N 615037.

Uniform engine testing program
Engine serial number 607594

C2 = -. 27825966E 01 NHR = 8900 rpm
C1 = -. 96055639E 00 T2AV = 288 K
C0 = 0. 10187426E 01 P2QAMB = 1. 3
◇ (P2AV = 51. 7), WAIR/WAIR' = . 99912E 00
WAIR (kg/s) = . 64903E 02
WAIR' (kg/s) = . 64960E 02

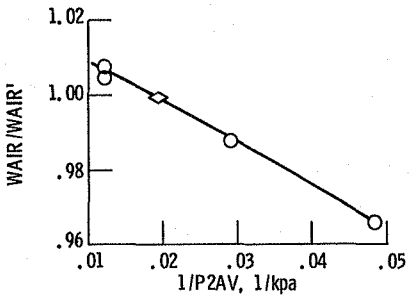

Figure 15. - Pressure influence.

Uniform engine testing program
engine serial number 607594

C2 = -. 30873194E-02 NHR = 8900 rpm
C1 = 0. 98351724E-02 P2AV = 82. 7 kpa
C0 = 0. 99243170E 00 T2AV = 288 K
◇ (P2QAMB = 1. 3), WAIR/WAIR' = . 10000E 01
WAIR (kg/s) = . 65384E 02
WAIR' (kg/s) = . 65384E 02

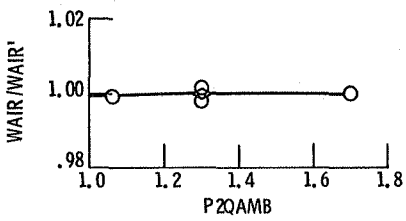

Figure 16. - Ram influence.

Uniform engine testing program
Engine serial number 607594

C2 = -. 88548304E-05 NHR = 8900 rpm
C1 = 0. 52067749E-02 P2AV = 82. 7 kpa
C0 = 0. 23490351E-00 P2QAMB = 1. 0
◇ (T2AV = 288. 0), FNR/FNR' = . 10000E 01
FNR (kn) = . 33366E 02
FNR' (kn) = . 33366E 02

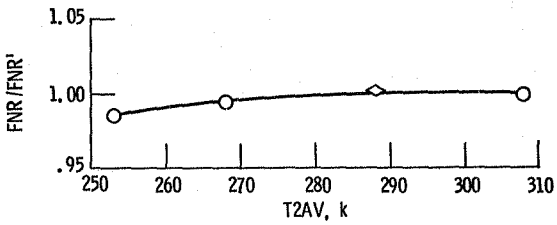

Figure 17. - Temperature influence.

Uniform engine testing program
Engine serial number 607594

C2 = -. 25023590E 02 NHR = 8900 rpm
C1 = 0. 31803265E 01 T2AV = 288 K
C0 = 0. 94647419E 00 P2QAMB = 1. 3
◇ (P2AV = 51. 7), FNR/FNR' = . 99863E 00
FNR (kn) = . 25466E 02
FNR' (kn) = . 25501E 02

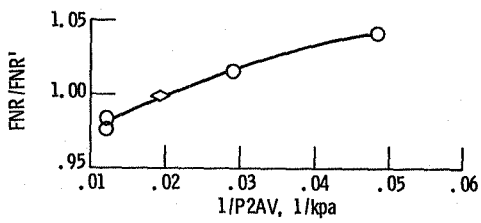

Figure 18. - Pressure influence.

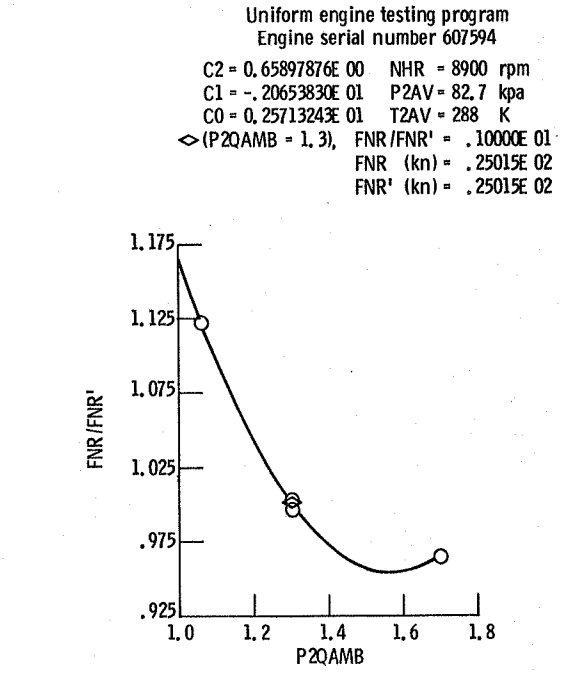

Figure 19. - Ram influence.

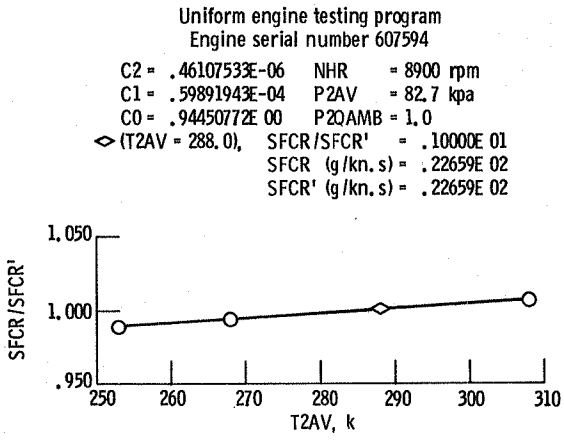

Figure 20. - Temperature influence.

Uniform engine testing program
Engine serial number 607594

C2 = .12302197E 02 NHR = 8900 rpm
C1 = .23905039E 01 T2AV = 288 K
C0 = .94955128E 00 P2QAMB = 1.3
◇ (P2AV = 51.7), SFCR/SFCR' = .10004E 01
SFCR (g/kn.s) = .30361E 02
SFCR' (g/kn.s) = .30349E 02

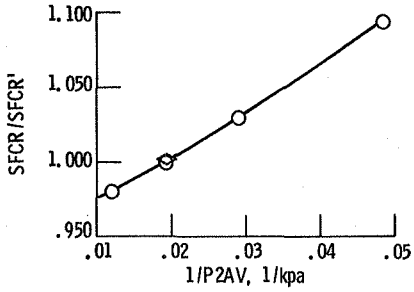

Figure 21. - Pressure influence.

Uniform engine testing program
Engine serial number 607594

C2 = -.53086585E 00 NHR = 8900 rpm
C1 = 0.16846066E 01 P2AV = 82.7 kpa
C0 = -.29282546E 00 T2AV = 288 K
◇ (P2QAMB = 1.3), SFCR/SFCR' = .10000E 01
SFCR (g/kn.s) = .29752E 02
SFCR' (g/kn.s) = .29752E 02

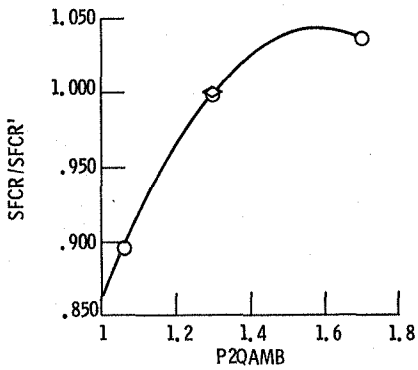

Figure 22. - Ram influence.

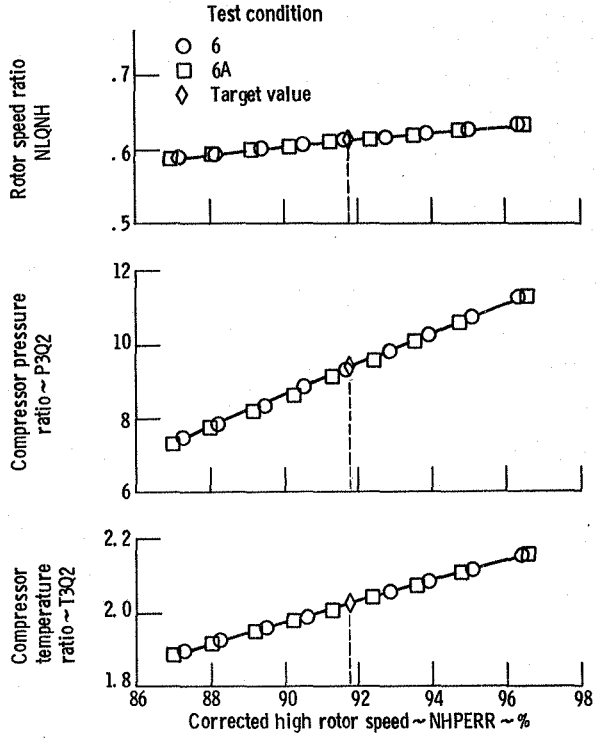

(a) Compressor performance.

Figure 23. - Standard AGARD engine performance plots (S/N 607594).

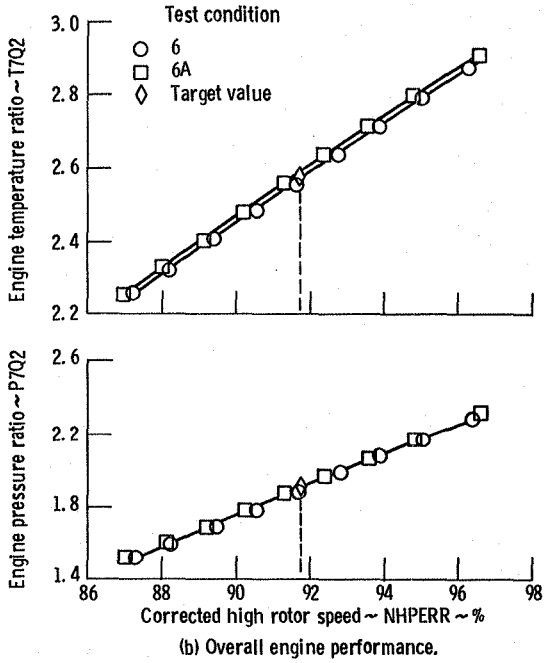

(b) Overall engine performance.

Figure 23. - Continued.

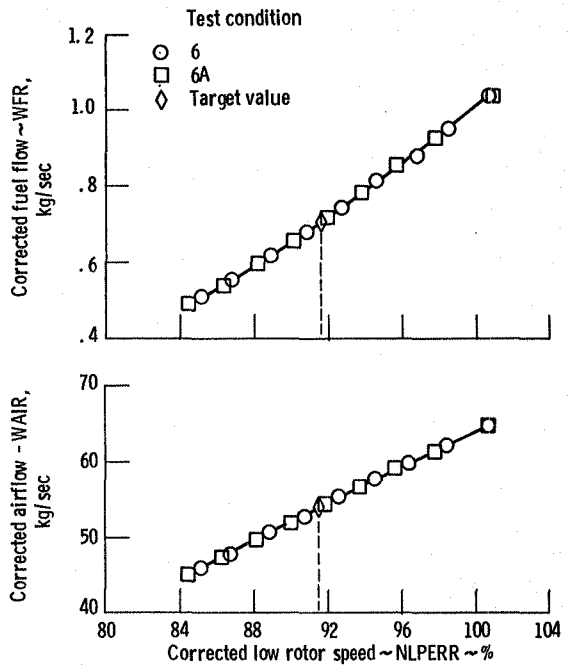

(c) Performance as a function of low rotor speed.

Figure 23. - Continued.

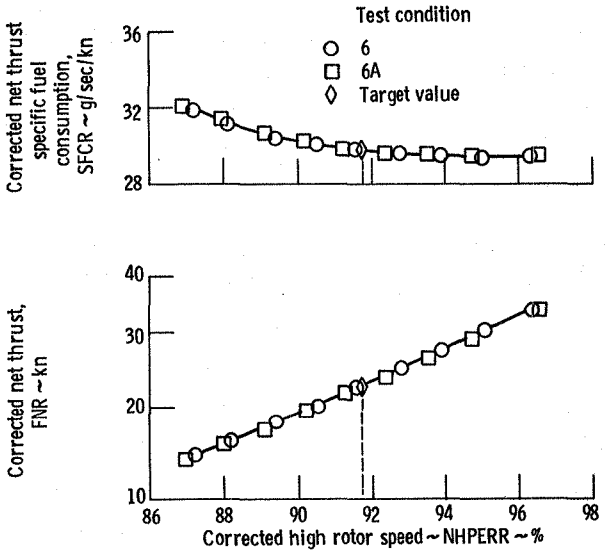

(d) Performance as a function of high rotor speed.

Figure 23. - Concluded.

Uniform engine testing program
Engine serial number 615037

C2 = -. 23745724E-05 NHR = 8900 rpm
C1 = 0. 11991754E-02 P2AV = 82.7 kpa
C0 = 0. 85344195E 00 P2QAMB = 1. 0
◇(T2AV = 288. 0), WAIR /WAIR' = . 10018E 01
WAIR (kg/s) = . 63766E 02
WAIR' (kg/s) = . 63648E 02

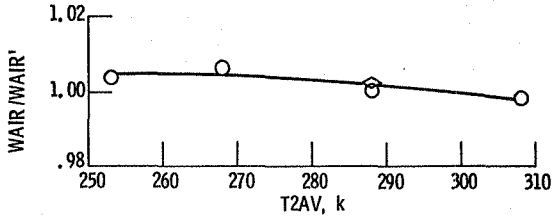

Figure 24. - Temperature influence.

Uniform engine testing program
Engine serial number 615037

C2 = -. 11597269E 02 NHR 8900 rpm
C1 = -. 49855417E 00 T2AV 288 K
C0 = 0. 10139751E 01 P2QAMB = 1. 3
◇(P2AV = 51. 7), WAIR /WAIR' = . 99999E 00
WAIR (kg/s) = . 64026E 02
WAIR' (kg/s) = . 64026E 02

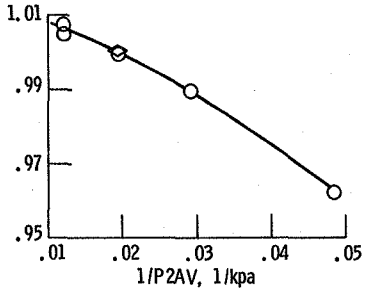

Figure 25. - Pressure influence.

C2 = -.51622070E-01 NHR = 8900 rpm
C1 = 0.16039115E 00 P2AV = 82.7 kpa
C0 = 0.87861669E 00 T2AV = 288 K
◇ (P2QAMB = 1.3), WAIR/WAIR' = .99988E 00
WAIR (kg/s) = .64419E 02
WAIR' (kg/s) = .64426E 02

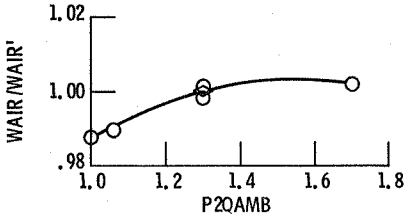

Figure 26. - Ram influence.

Uniform engine testing program
Engine serial number 615037

C2 = -.36245632E-06 NHR = 8900 rpm
C1 = 0.82235245E-04 P2AV = 82.7 kpa
C0 = 0.10098991E 01 P2QAMB = 1.0
◇ (T2AV = 288.0), FNR/FNR' = .10035E 01
FNR (kn) = .31672E 02
FNR' (kn) = .31561E 02

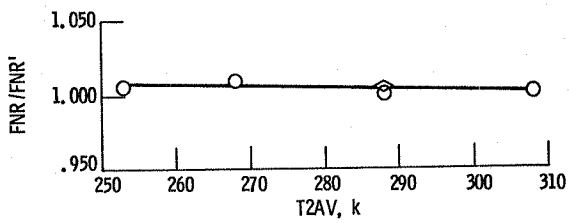

Figure 27. - Temperature influence.

Uniform engine testing program
Engine serial number 615037

C2 = -. 27760727E 02 NHR = 8900 rpm
C1 = 0. 32073259E 01 T2AV = 288 K
C0 = 0. 94578308E 00 P2QAMB = 1. 3
◇(P2AV = 51. 7), FNR/FNR' = .99743E 00
FNR (kn) = .24346E 02
FNR' (kn) = .24409E 02

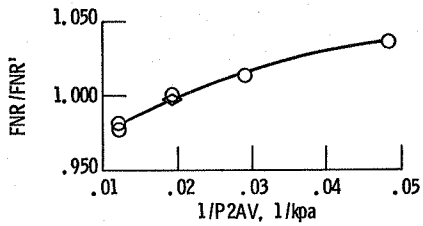

Figure 28. - Pressure influence.

Uniform engine testing program
Engine serial number 615037

C2 = 0. 12564230E 01 NHR = 8900 rpm
C1 = -. 38078661E 01 P2AV = 82. 7 kpa
C0 = 0. 38145237E 01 T2AV = 288 K
◇(P2QAMB = 1. 3), FNR/FNR' = .98765E 00
FNR (kn) = .23623E 02
FNR' (kn) = .23918E 02

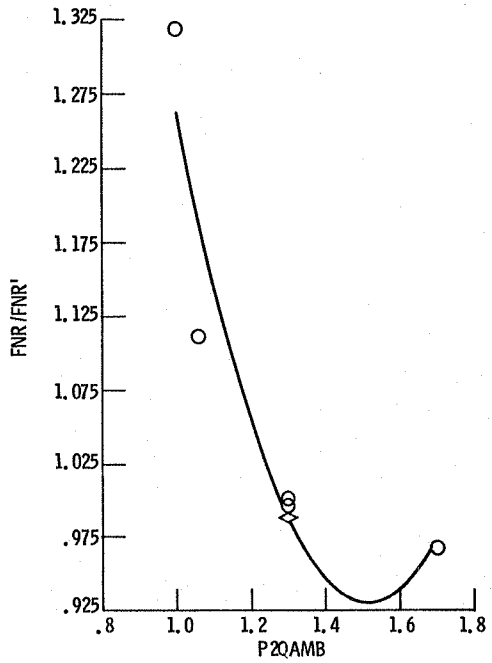

Figure 29. - Ram influence.

Uniform engine testing program
Engine serial number 615037

C2 = .24517095E-06 NHR = 8900 rpm
C1 = .12359538E-03 P2AV = 82.7 kpa
C0 = .94465345E 00 P2QAMB = 1.0
◇(T2AV = 288.0), SFCR/SFCR' = .10006E 01
SFCR (g/kn.s) = .22397E 02
SFCR' (g/kn.s) = .22384E 02

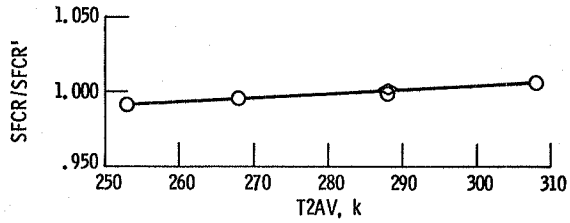

Figure 30. - Temperature influence.

Uniform engine testing program
Engine serial number 615037

C2 = .25316525E 01 NHR = 8900 rpm
C1 = .30055351E 01 T2AV = 288 K
C0 = .94482362E 00 P2QAMB = 1.3
◇(P2AV = 51.7), SFCR/SFCR' = .10039E 01
SFCR (g/kn.s) = .30277E 02
SFCR' (g/kn.s) = .30159E 02

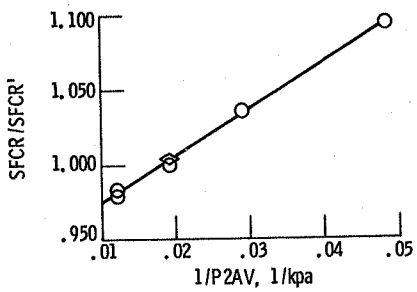

Figure 31. - Pressure influence.

Uniform engine testing program
Engine serial number 615037

C2 = -.94324911E 00 NHR = 8900 rpm
C1 = 0.28938065E 01 P2AV = 82.7 kpa
C0 = -.11602364E 01 T2AV = 288 K
◇ (P2QAMB = 1.3), SFCR/SFCR' = .10076E 01
SFCR (g/kn.s) = .29854E 02
SFCR' (g/kn.s) = .29628E 02

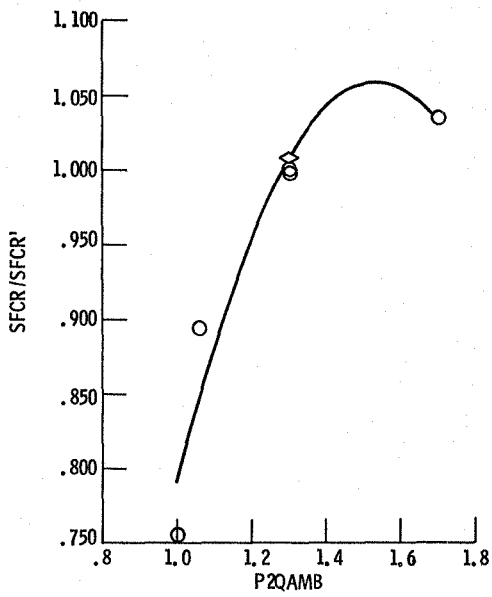

Figure 32. - Ram influence.

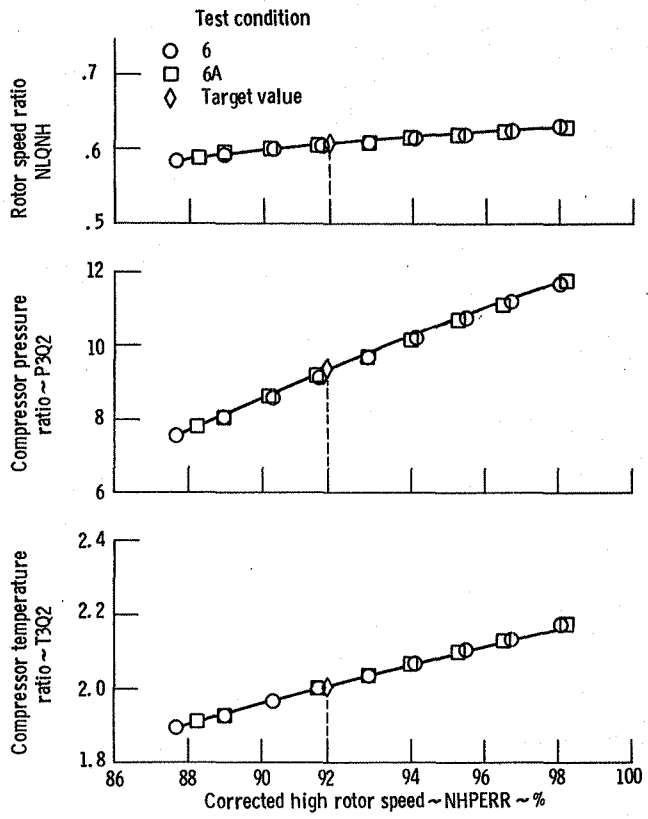

(a) Compressor performance.

Figure 33. - Standard AGARD engine performance plots (S/N 615037).

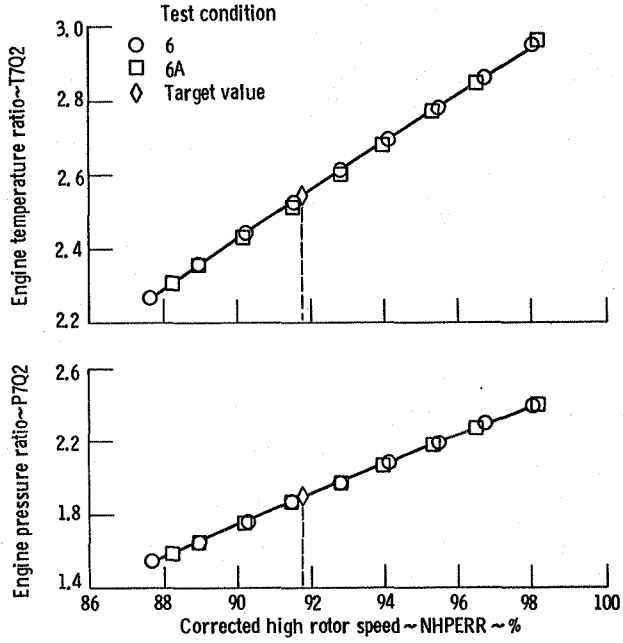

(b) Overall engine performance.

Figure 33. - Continued.

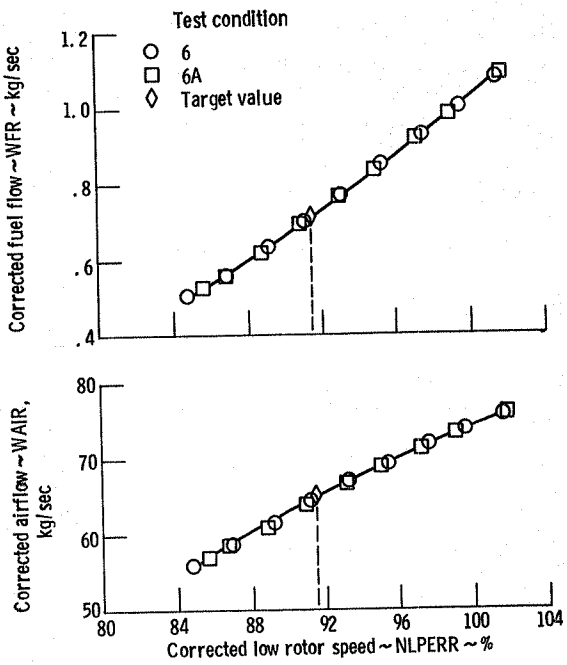

(c) Performance as a function of low rotor speed.

Figure 33. - Continued.

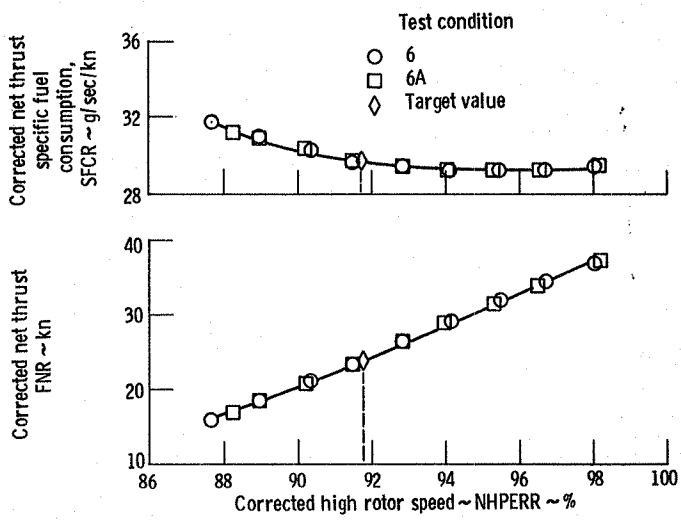

(d) Performance as a function of high rotor speed.

Figure 33. - Concluded.

1. Report No.	2. Government Accession No.	3. Recipient's Catalog No.
NASA TM-82978		

4. Title and Subtitle	5. Report Date
UNIFORM ENGINE TESTING PROGRAM PHASE I: NASA LEWIS RESEARCH CENTER PARTICIPATION	October 1982
	6. Performing Organization Code 505-32-6A
7. Author(s) T. Biesiadny, L. Burkardt, and W. Braithwaite	8. Performing Organization Report No. E-1407
	10. Work Unit No.
9. Performing Organization Name and Address National Aeronautics and Space Administration Lewis Research Center Cleveland, Ohio 44135	11. Contract or Grant No.
	13. Type of Report and Period Covered Technical Memorandum
12. Sponsoring Agency Name and Address National Aeronautics and Space Administration Washington, D.C. 20546	14. Sponsoring Agency Code

15. Supplementary Notes

Work performed for the Propulsion and Energetics Panel of the Advisory Group for Aerospace Research and Development (AGARD).

16. Abstract

The Propulsion and Energetics Panel, Working Group 15, of the Advisory Group for Aerospace Research and Development (AGARD) is sponsoring a Uniform Engine Testing Program (UETP). In this program, two jet engines will be tested under identical conditions in a variety of altitude and ground level facilities as a means to correlating these facilities. This report presents a summary of the results of testing two J57-19W turbojet engines in an altitude test facility at NASA Lewis Research Center, Cleveland, Ohio, U. S. A. in support of the AGARD panel's efforts.

17. Key Words (Suggested by Author(s))	18. Distribution Statement
Turbine engine testing Facility correlation Altitude test facilities	Unclassified - unlimited STAR Category 07

19. Security Classif. (of this report)	20. Security Classif. (of this page)	21. No. of Pages	22. Price*
Unclassified	Unclassified		

* For sale by the National Technical Information Service, Springfield, Virginia 22161

End of Document